Lyn expression in macrophages promotes TLR activation and restricts proliferation in an isoform-independent manner

Anders J. Lindstedt^{1,2}, Joseph T. Greene³, Yingzheng Xu⁴, Jesse W. Williams^{5,6}, and Tanya S. Freedman^{3,6,7*}

- ¹Medical Scientist Training Program, University of Minnesota, Minneapolis, MN 55455, United States ²Graduate Program in Microbiology, Immunology, and Cancer Biology, University of Minnesota, Minneapolis, MN 55455, United States
- ³Department of Pharmacology, University of Minnesota, Minneapolis, MN 55455, United States
- ⁴Graduate Program in Bioinformatics and Computational Biology, University of Minnesota, Minneapolis, MN 55455, United States
- ⁵Department of Integrative Biology and Physiology, University of Minnesota, Minneapolis, MN 55455, United States
- ⁶Center for Immunology, University of Minnesota, Minneapolis, MN 55455, United States
- ⁷Masonic Cancer Center, University of Minnesota, Minneapolis, MN 55455, United States
- *To whom correspondence should be addressed: tfreedma@umn.edu; 3-190 Wallin Medical Biosciences Building, 2101 6th Street SE, Minneapolis, MN 55455-0215

Conflict of Interest Disclosure

The authors declare that they have no conflicts of interest.

Abstract

Toll-like receptor (TLR) signaling is vital for antimicrobial macrophage function, and its dysregulation is associated with diseases such as lupus, multiple sclerosis, pulmonary fibrosis, and cancer. The Srcfamily kinase Lyn may have net activating or inhibitory effects on TLR signaling, yet distinct functions of the Lyn splice variants LynA and LynB in TLR signaling have not been investigated. We used isoformspecific Lyn knockout mice (LynAKO and LynBKO) to interrogate the contribution of each isoform to TLR signaling in bone-marrow-derived macrophages. Bulk RNA sequencing and cytokine analyses revealed that complete Lyn deficiency (Lyn^{KO}) dampened TLR4- and TLR7-induced inflammatory gene expression and production of tumor necrosis factor (TNF) but enhanced the expression of genes responsible for synthesizing the extracellular matrix and promoting proliferation. Despite reduced expression of total Lyn in single-isoform Lyn knockout BMDMs, expression of either LynA or LynB alone was sufficient to preserve a wild-type-like transcriptome at steady state and after treatment with the TLR7 agonist R848. However, LynA^{KO} and LynB^{KO} macrophages did have impaired TNF production in response to the TLR4 agonist lipopolysaccharide. Additionally, LynA^{KO} and LynB^{KO} macrophages were as hyperproliferative as Lyn^{KO} cells. These data suggest that Lyn promotes macrophage activation in response to TLR signaling and restrains aberrant proliferation and matrix deposition in a dose-dependent rather than isoform-specific manner.

Key Words: Src-family kinase, myeloid-cell signaling, transcriptomics, inflammation, extracellular-matrix remodeling

Summary Sentence: RNA sequencing and functional assays demonstrate that both LynA and LynB restrict macrophage proliferation and drive TLR-induced ECM-remodeling and inflammatory cytokine production.

Introduction

Macrophages play key roles in pathogen defense, wound healing, and tissue maintenance. Dysregulation of intracellular signaling is associated with infection¹, autoimmunity^{2,3}, fibrosis⁴⁻⁶, and cancer progression⁷⁻⁹. Yet mechanistic questions about how cells restrain pathological activation remain. Macrophage signaling can be initiated by transmembrane Toll-like receptors (TLRs), which detect extracellular ligands (e.g., TLR4) or endosomal ligands (e.g., TLR7)^{10,11}. TLRs respond to a variety of stimuli,

including bacterial membrane components such as lipopolysaccharide (LPS), RNA and DNA motifs such as GU-/AU-rich single-stranded RNA and unmethylated CpG DNA^{12,13}, and endogenous ligands such as high mobility group box 1 (HMGB1) and heat-shock proteins^{14,15}. Receptor ligation drives a diverse array of cellular responses: Inflammation results from the production of cytokines, such as tumor necrosis factor (TNF), interleukins (ILs), and interferons (IFNs). Chemokines, such as C-C motif chemokine ligands (CCLs) and C-X-C motif chemokine ligands (CXCLs), are secreted, recruiting immune cells¹⁶. TLRs also trigger cell proliferation via cyclin production¹⁷ and extracellular-matrix (ECM) remodeling via matrix metalloprotease (MMP) and collagen or laminin synthesis^{18,19}.

Signaling downstream of TLRs can be transduced via the adaptor protein MYD88, although TLR4 also signals through the adaptor protein TRIF^{20,16}. MYD88-dependent TLR4 signaling progress through MAPK and NF-κB pathways, culminating in the nuclear translocation of transcription factors NF-κB, CREB, and AP1-family members c-Jun and c-Fos²¹, whereas TRIF-dependent signaling effectuates interferon regulatory factor 3 (IRF3) translocation²¹. TLR7 drives NF-κB, AP-1, IRF5, and IRF7 translocation²². Even though these transcription factors regulate unique subsets of target genes, they converge on shared pathways. NF-κB induces inflammatory gene expression alone (e.g., *II1b*) and in cooperation with IRF5 (e.g., *Tnf*, *II6*, *II12*)²³. AP-1 drives the expression of ECM-remodeling genes (e.g., *Mmp9*), while also promoting *Tnf* and *II6* transcription²⁴. CREB regulates macrophage survival through *Serpinb2*, *Bcl2*, *II10*, and *Dusp* expression^{25,26}. IRF3 induces type-I IFN responses through *Ifnb1* expression and chemokine expression (e.g., *Cxcl10*, *Ccl5*)²⁷, whereas IRF7 induces *Ifna1* expression in addition to *Ifnb1*²⁸. Despite advances in our understanding of TLR signaling, the upstream regulatory factors that dictate selective activation and integration of these transcriptional programs remain incompletely defined.

The Src-family kinase (SFK) Lyn has emerged as a key modulator of TLR signaling, but the breadth of TLR-induced transcriptional programs that are regulated by Lyn in macrophages is unclear. Lyn can activate or inhibit TLR signaling²⁹⁻³¹, and cell-specific contributions in vivo are complex. Global Lyn knockout (Lyn^{KO}) mice develop a systemic lupus-like disease, characterized by myeloproliferation and splenomegaly, inflammation, autoreactive antibodies, and glomerulonephritis³²⁻³⁴. Progression to auto-immunity depends on the inflammatory environment created by IL-6, likely produced by hyperactive B cells³⁵, and B-cell-specific loss of Lyn is sufficient to drive the disease³⁶. Interestingly, dendritic cell (DC)-specific loss of Lyn is also sufficient to drive disease, rescued by secondary knockout of MYD88³⁷ or CARD9³⁸. Lyn can inhibit TLR signaling in myeloid cells, including DCs³⁷⁻³⁹ and macrophages^{40,41}, with Lyn^{KO} cells producing more type-I IFNs (IFNα and IFNβ), TNF, and IL-6 than wild-type (WT) cells. Lyn may phosphorylate IRFs, leading to their polyubiquitination and degradation and suppressing the production of type-I IFNs^{42,43}. However, this mechanism may be unique to classical DCs (cDCs), as Lyn^{KO} plasmacytoid DCs (pDCs) produce fewer inflammatory cytokines than WT³⁹. Moreover, macrophage-specific loss of Lyn does not induce autoinflammatory disease³⁸. Thus, the impact of Lyn on TLR-induced cellular responses may differ by cell type.

In support of potential activating functions of Lyn, overexpressing Lyn in mice also precipitates a lupus-like inflammatory disease⁴⁴, and antibody-secreting cells from human lupus patients can also have increased *LYN* expression⁴⁵. In myeloid cells, including macrophages, Lyn activates inflammatory signaling pathways^{46,47}. Specifically, TLR-driven production of inflammatory cytokines is dependent on Lyn⁴⁸⁻⁵¹. Given the multifunctional nature of Lyn in cell signaling and inflammatory disease and the diverse signaling programs controlling TLR activation and cellular responses, the role of Lyn in macrophage TLR signaling cascades requires further investigation.

Lyn RNA is alternatively spliced to produce two isoforms, LynA and LynB, which differ by an insert in the N-terminal unique region of LynA⁵². LynA is uniquely regulated through polyubiquitination and degradation^{53,54} and may be the dominant driver of mast-cell degranulation⁵⁵. Conversely, overexpressed LynB associates more with inhibitory signaling proteins⁵⁵. Our group generated isoform-specific LynA^{KO} and LynB^{KO} mice and discovered that LynB^{KO} and female LynA^{KO} mice develop lupus with age³⁴. We found myeloproliferation and increased expression of CD11c on macrophages in LynA^{KO} and LynB^{KO}

mice. Interestingly, female LynA^{KO} macrophages expressed higher amounts of the activation marker CD80/86 relative to LynA^{KO} male and WT cells. Still, few studies have examined isoform-specific functions of Lyn in macrophages, and the roles of LynA or LynB in TLR signaling were previously unknown.

To investigate specific functions of LynA and LynB in macrophage TLR responses, we performed RNA sequencing and cytokine analyses in single-isoform and complete Lyn^{KO} bone-marrow-derived macrophages (BMDMs) at rest or treated with TLR4 or TLR7 agonist. While a complete loss of Lyn impaired TLR4- and TLR7-induced expression of inflammatory genes and production of TNF protein, expression of either LynA or LynB was sufficient to preserve WT-like transcriptional responses and cytokine production. However, LynA^{KO} and LynB^{KO} macrophages did have partially impaired TNF production in response to TLR4 stimulation. Additionally, all Lyn-deficient macrophages were hyperproliferative, including isoform-specific knockout cells. These data suggest that Lyn promotes macrophage activation downstream of TLRs and restrains aberrant proliferation in a dose-dependent rather than isoform-specific manner.

Materials and Methods

Human Subjects

No human subjects or samples were used for this study, so institutional review (IRB approval) by the University of Minnesota for human subjects was not required.

Mouse strains and housing

C57BL/6-derived LynA^{KO}, LynB^{KO}, and Lyn^{KO} mice have been described previously^{33,34}. The LynA^{KO} and LynB^{KO} mice used for this study were hemizygous F1 progeny of single-isoform and Lyn^{KO} breeders (LynA^{-/-}LynB^{+/-} and LynB^{-/-}LynA^{+/-}) to ensure WT-like expression of the remaining isoform³⁴. Animal use was compliant with University of Minnesota/American Association for Accreditation of Laboratory Animal Care and National Institutes of Health policy, under Animal Welfare Assurance number A3456-01 and Institutional Animal Care and Use Committee protocol number 2209-40372A. Mice were housed in a specific-pathogen-free facility under the supervision of a licensed Doctor of Veterinary Medicine and supporting veterinary staff. Breeding and experimental mice were genotyped via real-time polymerase chain reaction (Transnetyx, Memphis, TN). Genotyping was confirmed by immunoblotting for Lyn, when appropriate.

Generation of BMDMs

BMDMs were generated as described previously^{53,56}. Briefly, bone marrow was isolated from femora and tibiae of mice, treated in hypotonic solution to remove erythrocytes, seeded in non-tissue-culture-treated polystyrene plates (CELLTREAT, Ayer, MA; Cat. 229653), and cultured at 37°C, 10% CO₂ in Dulbecco's Modified Eagle's Medium (DMEM, Corning Mediatech, Manassas, VA; Cat. 10-017-CM) with final concentrations of 10% heat-inactivated fetal bovine serum (FBS, Omega Scientific, Tarzana, CA; Cat. FB-11), 1 mM sodium pyruvate (Corning Mediatech; Cat. 25-000-CI), 6 mM L-glutamine (Gibco, Grand Island, NY; Cat. 25030-081), 1% Penicillin-Streptomycin (179 and 172 μM, respectively, Sigma-Aldrich, St. Louis, MO; Cat. P4333-100ML), and 5% CMG14-12 supernatant as a source of macrophage colony-stimulating factor (M-CSF). After 7 d culture with medium refreshment, BMDMs were harvested with enzyme-free cell dissociation buffer (Gibco, Grand Island, NY; Cat. 13150-016), washed with phosphate-buffered saline (PBS, Cytiva, Logan, UT; Cat. SH30256.01), and counted for replating.

Treatment with TLR agonists

BMDMs were resuspended in culture medium without M-CSF, replated, and rested overnight. Cells were then treated with medium alone (-) or with 2 ng/ml LPS from *S. Minnesota* R595 (List Biological Laboratories, Campbell, CA; Cat. 304) or 20 ng/ml R848 (InvivoGen, San Diego, CA; Cat. tlrl-r848-1). Signaling was quenched at endpoints described below, and samples were stored at -80°C.

RNA sequencing

After 2 h treatment, cells were washed in PBS and lysed in TRIzol (Thermo Fisher Scientific, Waltham, MA; Cat. 15596018). RNA was isolated via chloroform extraction followed by RNeasy Mini Kit (Qiagen, Hilden, Germany; Cat. 74104). Samples from 4 mice of each genotype (2 male, 2 female) were subjected to poly-A selection to isolate mRNA and then bulk, next-generation sequencing (Illumina NovaSeq 6000 platform, performed by Azenta Life Sciences, South Plainfield, NJ). Sequence reads (17.5-27 x 10⁶ per sample) were trimmed using *Trimmomatic v.0.36* and mapped to the ENSEMBL *Mus musculus* GRCm38 reference genome using *STAR aligner v.2.5.2b*. Unique hit counts were determined using *featureCounts* in the *Subread* package *v.1.5.2* for downstream analysis of differential gene expression.

DESeq2 analysis

Genes were filtered in R v.4.4.3 to retain only those with \geq 10 counts in \geq 3 of the 4 biological replicates within any genotype/treatment. Differential expression analysis was performed using the DESeg2 package v.1.46.0, with samples grouped by genotype and treatment in the design formula (~ Group). Variance-stabilizing transformation (VST) was applied to normalized counts for visualization and unsupervised clustering. Principal component analysis (PCA) was conducted on the 500 most variable genes across all samples using the prcomp function in the stats package of base R, and results were visualized using the gaplot function in the gaplot2 package v.3.5.2, with samples colored by genotype and treatment. Differentially expressed genes (DEGs) were identified using the results function in DESeq2, and pairwise comparisons between genotypes within each treatment condition were performed. The results function in DESeq2 uses the Wald test to calculate log2(fold-changes) and p-values and the Benjamini-Hochberg False Discovery Rate correction to calculate adjusted p-values. Genes were defined as differentially expressed if they met both a Benjamini–Hochberg adjusted p-value <0.05 and an absolute fold-change >1.5. DESeg2 output was annotated using ENSEMBL gene IDs mapped to gene symbols using the *biomaRt* package *v.2.62.1*. To assess shared and condition-specific differential gene expression between genotypes, Venn diagrams were created using the venn.diagram and draw.triple.venn functions in the VennDiagram package v.1.7.3, and plots were rendered using the grid.draw function in the grid package of base R. VST-normalized gene expression was visualized using the pheatmap package v.1.0.12, with row-wise scaling, Euclidean clustering of genes, and a scaled color palette to represent relative expression levels. The total distribution of differential gene expression between genotypes was visualized with volcano plots generated using the ggplot function in ggplot2, with $\log_2(\text{fold-change})$ on the x axis and $-\log_{10}(\text{adjusted }p\text{-value})$ on the y axis. Threshold lines were included to denote significance cutoffs (adjusted p-value <0.05 and an absolute fold-change >1.5), and colorcoding was applied to distinguish relative expression changes, with red indicating significantly increased expression, blue indicating significantly decreased expression, and all others in gray.

Gene set enrichment analysis (GSEA)

The GSEA desktop application v.4.4.0 (Broad Institute, Cambridge, MA) was used to evaluate pathway-level differences between genotypes at steady state and after LPS or R848 treatment. VST-normalized gene-expression matrices (generated from DESeq2) were used as input, with genes ranked by signal-to-noise. Comparisons were made between genotypes within each treatment condition using phenotype-based permutation (n = 1000). Gene identifiers were mapped from ENSEMBL IDs to official gene symbols using the MSigDB v.2025.1 Mm.chip annotation file. Enrichment testing was performed using 29 hallmark gene-sets of interest or 16 curated ECM-related gene sets. Gene sets with <15 or >500 genes were excluded. Enrichment was weighted, and results were filtered and visualized using default GSEA settings. Significant gene-set enrichment was defined by a nominal p-value <0.1.

qRT-PCR analysis

After 2-8 h treatment and cell lysis, RNA from TRIzol lysates was converted into complementary DNA via qScript cDNA Synthesis (QuantaBio, Beverly, MA; Cat. 95047-500). Products were diluted 1:10 in

ultrapure water and subjected in technical triplicate to qRT-PCR using QuantStudio 3 PCR (Thermo Fisher Scientific) with PerfeCTa SYBR Green SuperMix (Thermo Fisher Scientific; Cat. 4385616). For each reaction, an equivalent amount of water in triplicate was substituted for cDNA as a negative control. Threshold-cycle (Ct) values were normalized to the housekeeping gene *Cyclophillin*, and mRNA fold changes were calculated using the ΔΔCt method⁵⁷. Primer sequences (forward/reverse 5'-3'): *Cyclophillin* (TGCAG GCAAA GACAC CAATG / GTGCT CTCCA CCTTC CGT), *Tnf* (CCTCT TCTCA TTCCT GCTTG TG / TGGGC CATAG AACTG ATGAG AG), *II1b* (GCAAC TGTTC CTGAA CTCAA CT / ATCTT TTGGG GTCCG TCAAC T), *II6* (TGTTC TCTGG GAAAT CGTGG A / CTGCA AGTGC ATCATC GTTGT), *II12b* (AGTGT GAAGC ACCAA ATTAC TC / CCCGA GAGTC AGGGG AACT).

Immunoblotting and quantification

After up to 30 min treatment, protein phosphorylation was assessed via immunoblotting, as described previously⁵⁶. Briefly, BMDMs were collected, lysed with SDS sample buffer, sonicated, treated with dithiothreitol, and boiled. Approximately 3.5 x 10⁴ cell equivalents were run in each lane of a 7% Nu-PAGE tris-acetate gel (Invitrogen, Carlsbad, CA; Cat. EA03585BOX) and transferred to an Immobilion-FL polyvinylidene difluoride membrane (EMD Millipore, Burlington, MA; Cat. IPFL00010). REVERT 700 Total Protein Stain (LI-COR Biosciences, Lincoln, NE; Cat. 926-11021) was used to assess whole-lane protein content. After reversal of the total protein stain, membranes were treated for 1 h with Intercept Blocking Buffer (LI-COR Biosciences; Cat. 927-60001) and then incubated with appropriate primary antibodies overnight at 4 °C, followed by incubation with near-infrared secondary antibodies for 1 h at room temperature. Blots were visualized using an Odyssey CLx near-infrared imager (LI-COR Biosciences) and analyzed using ImageStudio Software (LI-COR Biosciences). Signals were backgroundsubtracted and corrected for whole-lane protein content. Values were then normalized to the untreated control for each replicate and genotype. Primary Antibodies: P-IKKα/β (Cell Signaling Technology (CST), Danvers, MA; Cat. 2697S), P-AKT (CST, Cat. 9271S), P-JNK (CST, Cat. 4668T), P-ERK (CST, Cat. 4370S), ERK (CST, Cat. 9107S). Secondary Antibodies: Donkey anti-mouse IgG 680RD (LI-COR Biosciences, Cat. 926-68072), Donkey anti-rabbit IgG 700CW (LI-COR Biosciences, Cat. 926-32213).

Quantification of TLR protein

BMDMs were resuspended in flow-cytometry buffer comprising PBS, 2% heat-inactivated FBS, and 2 mM ethylenediaminetetraacetic acid, and cells were stained for viability with Ghost Dye Red 780 (Tonbo Biosciences, San Diego, CA; Cat. 13-0865-T500). Cells were then blocked with Fc Shield, Clone 2.4G2 (Tonbo Biosciences; Cat. 70-0161-U500) and stained for surface TLR4 with BV650 anti-mouse CD284/MD-2 Complex, Clone MTS510 (BD Biosciences, Franklin Lakes, NJ; Cat. BDB740615) in flow-cytometry buffer. Cells were then washed and treated with Cytofix/Cytoperm (BD Biosciences; Cat. 554722), washed with BD Perm/Wash buffer (BD Biosciences; Cat. 554723), and stained for intracellular TLR7 with PE anti-mouse CD287, Clone A94B10 (BioLegend, San Diego, CA; Cat. 160003). Flow cytometry was performed on a BD LSRFortessa or LSRFortessa X-20 cytometer, and data were analyzed using FlowJo software v.10.9.0 (FlowJo, Ashland, OR).

Quantification of cell proliferation

BMDMs were generated from 3 mice of each genotype and resuspended in culture medium without M-CSF. PBS-diluted CellTrace Violet (CTV, Thermo Fisher Scientific; Cat. C34557) was added to cell suspensions. Cells were washed and resuspended in culture medium with M-CSF, plated in untreated polystyrene plates, and incubated 96 h at 37°C in 10% CO₂. Cells were then washed, stained for viability, and analyzed via flow cytometry, as described above. The *Proliferation Modeling* function in FlowJo was used to quantify division within the "Live" cell gate.

Enzyme-linked immunosorbent assay (ELISA)

TNF secretion by BMDMs over 24 h was analyzed using the mouse TNF DuoSet ELISA Kit according to manufacturer's instructions, with a 7-point standard curve (R&D Systems, Minneapolis, MN; Cat. DY410). A Tecan Infinite 200 PRO was used to determine the absorbance of each well at 450 nm

(A₄₅₀), with 540-nm background correction. The average zero standard was subtracted from the average of each standard or sample. A standard curve was created by plotting log(A₄₅₀) by log[standard] and applying linear regression with GraphPad Prism *v.9.1.2* (GraphPad Software, Boston, MA)..

Graphing and statistical analysis

Graphing and statistics were performed using GraphPad Prism software. In scatter plots and bar graphs, data are presented as mean ± standard deviation (SD) or standard error of the mean (SEM) as indicated, with significance assessed via two-way ANOVA with Tukey's multiple comparisons test. *p*-value <0.05 *, <0.01 ***, <0.001 ****, <0.0001 ****, *ns* indicates no significant differences. Outlier analyses were performed on ELISA data using unbiased robust regression and outlier elimination (ROUT) with Q=1%. *n* indicates the number of biological replicates, where each replicate represents cells from an individual mouse. In graphs depicting proliferation or ELISA data, squares indicate cells derived from male mice, and circles indicate cells derived from female mice.

Results

Expression of either LynA or LynB in macrophages is sufficient to maintain a WT-like transcriptome

We performed RNA sequencing on WT, LynA^{KO}, LynB^{KO}, and total Lyn^{KO} BMDMs following a 2-hour incubation in medium alone or with the TLR4 agonist LPS or TLR7 agonist R848. PCA revealed that treatment with either LPS or R848 induced profound transcriptional changes that were more dominant in defining the transcriptome than the cell genotype. (**Fig. 1A**).

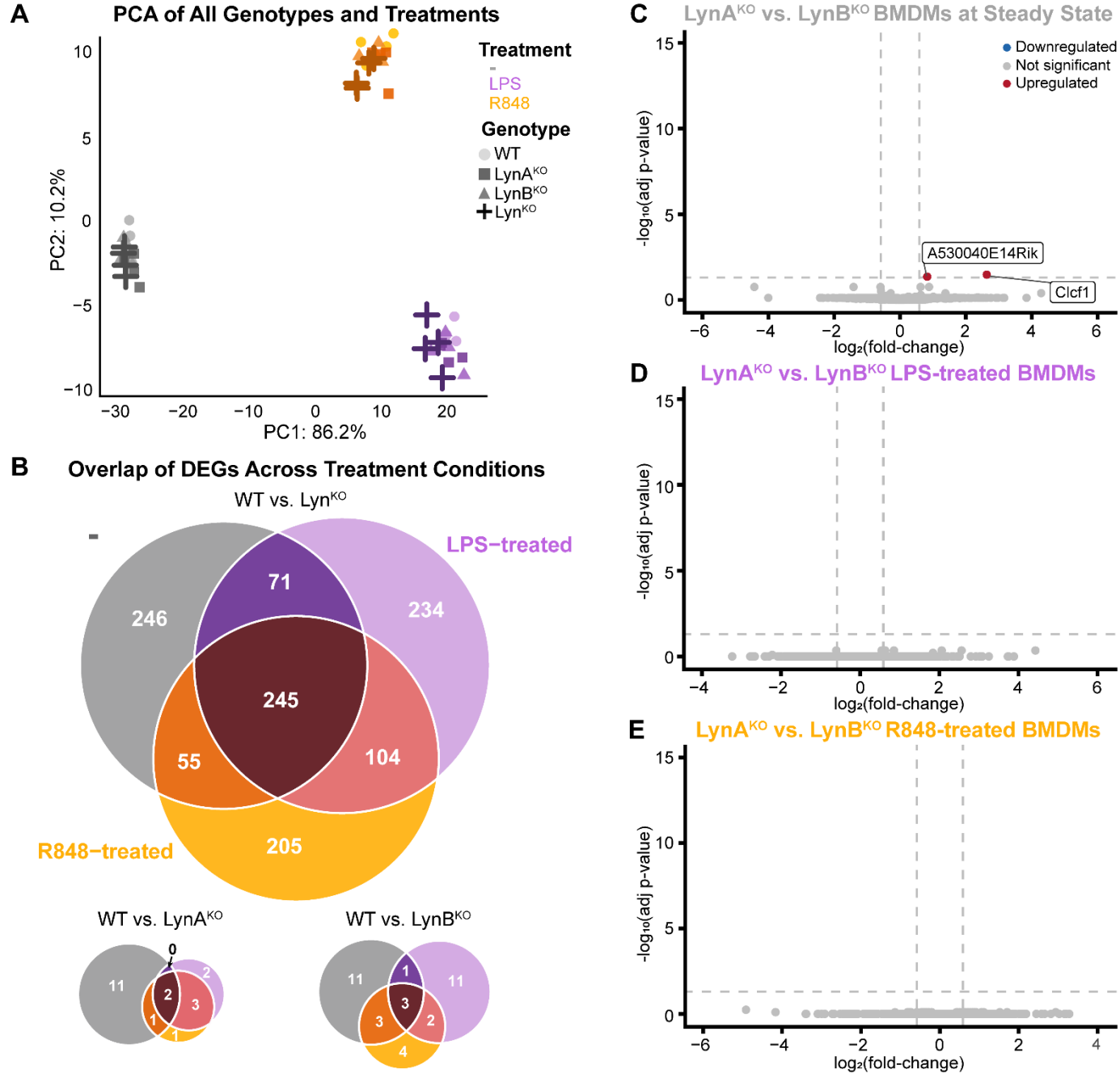


Figure 1. Expression of either LynA or LynB alone is sufficient to reverse transcriptomic dysregulation induced by complete Lyn knockout in BMDMs. (A) PCA of bulk RNA sequencing data from WT (circle), LynA^{KO} (square), LynB^{KO} (triangle) or total Lyn^{KO} (plus) BMDMs treated 2 h with medium alone (-, gray), 2 ng/ml LPS (purple), or 20 ng/ml R848 (orange); cells were prepared independently from 4 individual mice (2 male and 2 female from each genotype) and treated separately (n=4). Data set: 500 most variable genes, calculated from VST-normalized hit counts using prcomp in R. PC1 and PC2 account for 96.4% of the total variance. (B) Overlap of significant DEGs between Lyn knockout and WT BMDMs across all treatment conditions. DEGs were calculated from pairwise comparisons using DESeq2 and defined by an absolute fold change >1.5 and an adjusted p-value <0.05. (C-E) Volcano plots highlighting DEGs between LynA^{KO} and LynB^{KO} BMDMs at (C) steady state and after (D) LPS or (E) R848 treatment.

However, Lyn^{KO} BMDMs were shifted closer than other genotypes to steady-state transcriptomic profiles. Many genes were differentially expressed (DEGs) according to treatment condition and genotype (Fig. 1B). Although LynA and LynB are differentially regulated posttranscriptionally^{53,54} and contribute differentially to autoimmune disease and monocyte/macrophage phenotypes³⁴, the transcriptional profiles of LynA^{KO} and LynB^{KO} BMDMs were almost identical to each other at steady state (Fig. 1C) and indistinguishable after treatment with TLR4 agonist (Fig. 1D) or TLR7 agonist (Fig. 1E). Therefore, we focused subsequent analyses on differences between each Lyn knockout and WT.

Even in the absence of TLR stimulation, Lyn^{KO} and WT BMDMs had >600 DEGs, reflecting the pivotal role of Lyn in regulating the macrophage steady state (**Fig. 2A**). Whereas the complete loss of Lyn led to significant upregulation or downregulation of many gene products, loss of either LynA or LynB alone had modest, intermediate effects (**Fig. 2B**). Lyn^{KO} BMDMs had reduced expression of genes encoding pro-inflammatory cytokines, such as *Tnf*, *Il1a*, and *Il1b*, and chemokines, such as *Ccl2*, *Ccl3*, *Ccl7*, and *Cxcl10* (**Fig. 2C**). Complete loss of Lyn also affected expression of genes encoding proteolytic enzymes and structural proteins, with decreased *Mmp8*, *Mmp12*, and *Mmp14* and increased *Col4a1*, *Col4a2*, and *Lama3*. Lyn^{KO} cells also had increased expression of *Top2a*, *Tk1*, *Stmn1*, *Odc1*, and *Lig1*, which encode critical enzymes for DNA synthesis, replication, and repair, as well as cell-cycle progression and mitosis.

There were few differences in the steady-state transcriptomes of WT BMDMs and LynA^{KO} (Fig. 2D) or LynB^{KO} (Fig. 2E). However, LynA^{KO} cells had reduced expression of *Ccl2*, *Ccl7*, and *Mmp14*, and both LynA^{KO} and LynB^{KO} cells had increased expression of *Col4a1* (Sup. Fig. 1A). These findings suggest that Lyn^{KO} BMDMs in culture already have transcriptomic changes that alter their function and responses to stimuli. Expression of either Lyn isoform, however, is sufficient to restore a WT-like transcriptome in resting cells.

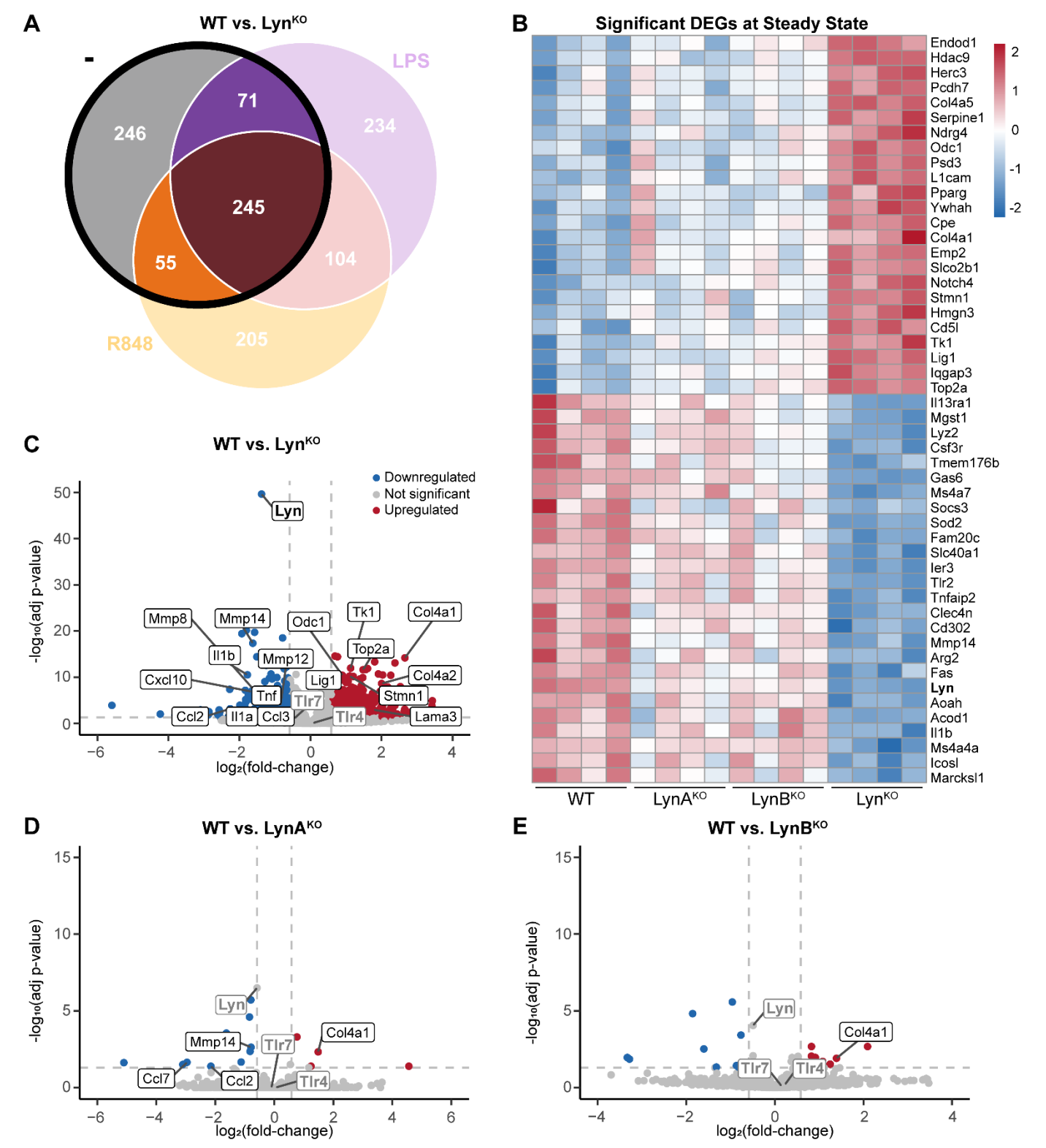


Figure 2. At steady state, LynKO BMDMs have decreased expression of genes encoding cytokines and proteases and increased expression genes encoding structural proteins and cell-cycle machinery. (A) Venn diagram highlighting DEGs in WT and Lyn^{KO} BMDMs at steady state (medium alone, -). (B) Heat map showing relative expression of the 50 highest-significance DEGs in WT and Lyn knockout BMDMs at steady state. Heat maps in this and other figures were generated using pheatmap in R to show z scores of VST-normalized hit counts for each sample relative to the mean count for each gene across all samples (red: increased, blue: decreased). The arrangement of rows was generated using hierarchical clustering by Euclidian distance. (C-E) Volcano plots highlighting DEGs at steady state between WT BMDMs and (C) Lyn^{KO}, (D) LynA^{KO}, or (E) LynB^{KO}. DEGs were calculated from pairwise comparisons using DESeq2 and defined by an absolute fold-change >1.5 and an adjusted p-value <0.05.

Few receptor-specific transcriptional differences distinguish TLR4 and TLR7 signaling in macrophages

We assessed the highest-significance DEGs in WT BMDMs after a 2-hour treatment with medium alone or with the TLR4 agonist LPS or the TLR7 agonist R848. For these studies, we chose agonist doses that induced comparable upregulation of *Tnf* in WT BMDMs (**Sup. Fig. 2A inset**). Consistent with previous studies^{58-61,10}, treatment with either LPS or R848 drove upregulation of genes encoding pro-inflammatory cytokines (e.g., *Tnf*, *Il1a*, *Il6*, *Il12a*, *Il12b*, *Il23a*, *Acod1*), chemokines (e.g., *Ccl4*, *Ccl5*, *Cxcl1*, *Cxcl2*, *Cxcl3*), mitogens (e.g., *Csf2*), and matrix metalloproteases (e.g., *Mmp13*, **Fig. 3A, Sup. Fig. 2A)**.

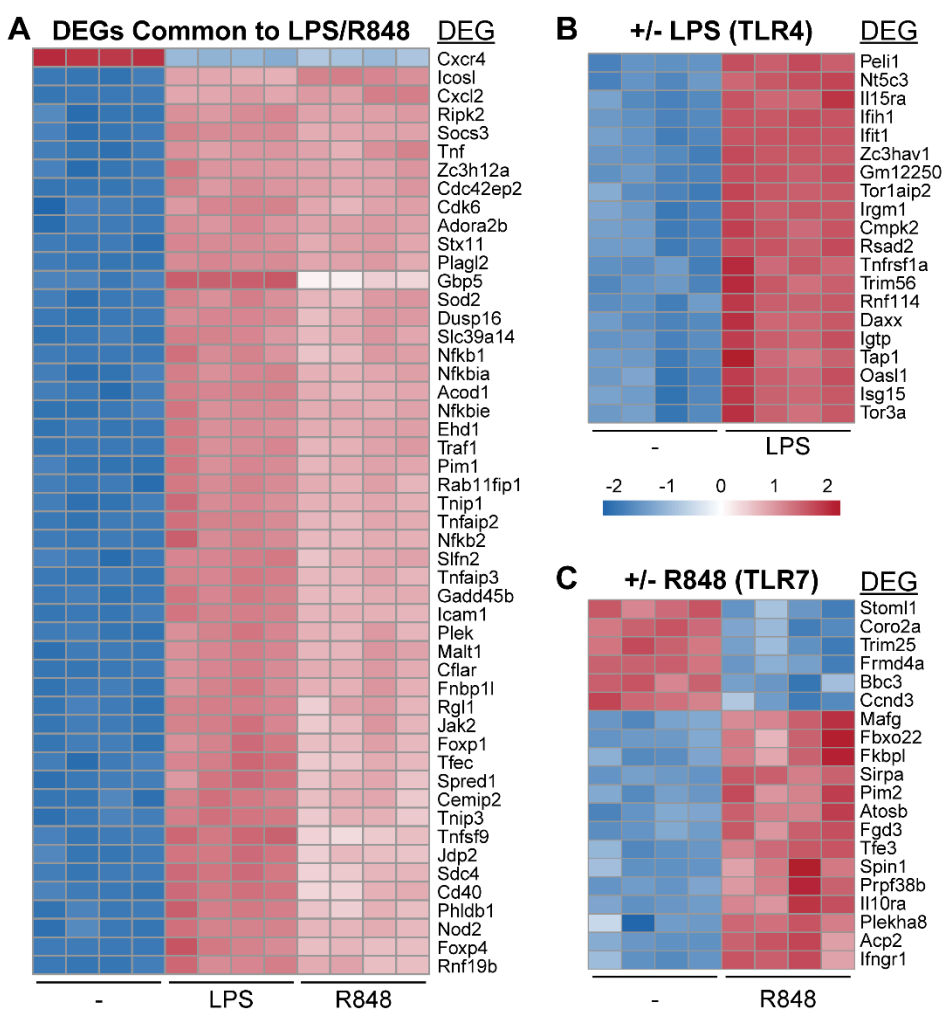


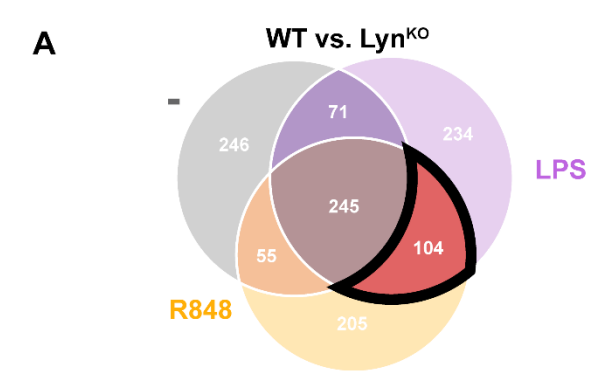
Figure 3. WT BMDM transcriptomes have some distinct features after LPS and R848 treatment. (A) Heat map of the 50 highest-significance DEGs common to LPS-treated and R848-treated WT BMDMs compared to cells in medium alone. (B,C) Heat maps of the 20 highest-significance DEGs unique to (B) LPS treatment or (C) R848 treatment. Heat maps and DEGs were compiled as described in Fig. 2.

Either TLR pathway also drove downregulation of *Cxcr4*, which, in vivo, leads to myeloid-cell egress from the bone marrow into peripheral blood⁶². Focusing on transcriptomic differences uniquely induced by the TLR4 or TLR7 pathway, we found that LPS treatment drove interleukin and chemokine genes, such as *Il33* and *Cxcl9*, and triggered a greater degree of gene induction than R848, with more upregulation of *Cxcl10* (**Fig. 3B, Sup. Fig. 2B**). Macrophage-produced CXCL9 and CXCL10 are critical for anti-tumor T-cell infiltration and response to immune checkpoint blockade⁶³. Interestingly, R848 uniquely induced downregulation of several genes, including *Ankrd6*, *Mcc*, *Trim15*, and *Trim25* (**Fig. 3C, Sup. Fig. 2C**). TRIM25 shifts the balance of signaling-pathway activation in macrophages, favoring MAPK and anti-inflammatory signaling over NF-κB activation⁶⁴. R848 also drove upregulation of *Ifngr1*, *Il10ra*, and *Sirpa*. A delicate balance of signaling through the IL10 receptor and SIRPα regulates inflammation-induced phagocytosis of healthy cells in macrophages⁶⁵. Despite these receptor-specific

differences in gene induction, most of the significant transcriptomic changes induced by TLR4 or TLR7 stimulation of WT BMDMs are shared between these two receptors.

Lyn deficiency broadly impacts TLR-induced gene transcription in macrophages

Neither mRNA expression of TLR-associated proteins (**Sup. Fig. 3A**), nor the protein levels of TLR4 and TLR7 (**Sup. Fig. 3B,C**) were altered by Lyn knockout, enabling a direct comparison of TLR signaling responses. We therefore compared the transcriptomes of WT, LynA^{KO}, LynB^{KO}, and Lyn^{KO} BMDMs treated with TLR4 or TLR7 agonists. LPS or R848 treatment of Lyn^{KO} BMDMs led to dysfunctional modulation of 371 genes that were also dysregulated at steady state (e.g., *Tnf, II1a, II1b, CcI2, CcI3, CxcI10, Mmp8, Mmp12, Mmp14, CoI4a1, CoI4a2, Lama3*). However, Lyn^{KO} BMDMs failed to modulate the expression of 104 additional gene products after either TLR4 or TLR7 stimulation (**Fig. 4A**), including failed upregulation of pro-inflammatory factors (e.g., *II12b, II23a, P2ry13, P2ry14, Pilrb1, Tnfsf15*) and chemokine-encoding genes (e.g., *CcI22, CcI24*), coupled with supraphysiological induction of inflammation-suppressing genes (e.g., *Traip, Sigirr, Fig. 4B*).



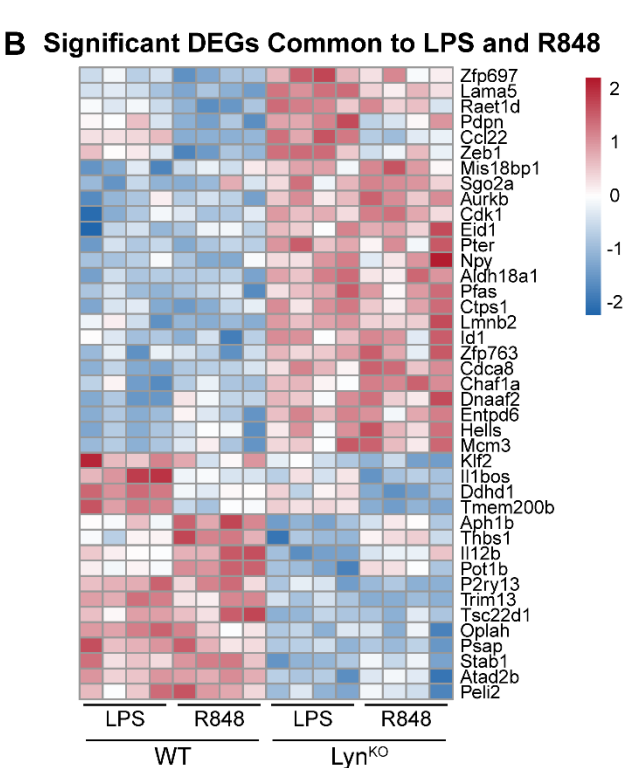


Figure 4. LynKO BMDMs have impaired upregulation of a pro-inflammatory transcriptome after TLR stimulation. (A) Venn diagram defining the subset of genes similarly upregulated or downregulated after either LPS or R848 treatment of WT and Lyn^{KO} BMDMs. **(B)** Heat map showing the highest-significance DEGs in the subset defined in (A). the 41 DEGs found in common among the 50 highest-significance DEGs between Lyn^{KO} and WT BMDMs after LPS or R848 treatment. Heat maps and DEGs were compiled as described in Fig. 2.

Additionally, Lyn^{KO} cells had impaired induction of genes encoding matrix metalloproteases (e.g., *Mmp13*) and enhanced induction of genes encoding structural proteins (e.g., *Lama5, Plod2, Fgl2*). Again, these defects were rescued by expression of either LynA or LynB, although LynA^{KO} and LynB^{KO} BMDMs did have increased *Lama5* expression, and LynB^{KO} BMDMs had increased *Notch4* expression (**Sup. Fig. 1B**).

To assess TLR-specific requirements for Lyn, we examined LPS-specific and R848-specific DEGs in WT and Lyn^{KO} BMDMs. We identified 234 DEGs found only in LPS-treated samples **(Fig. 5A)**.

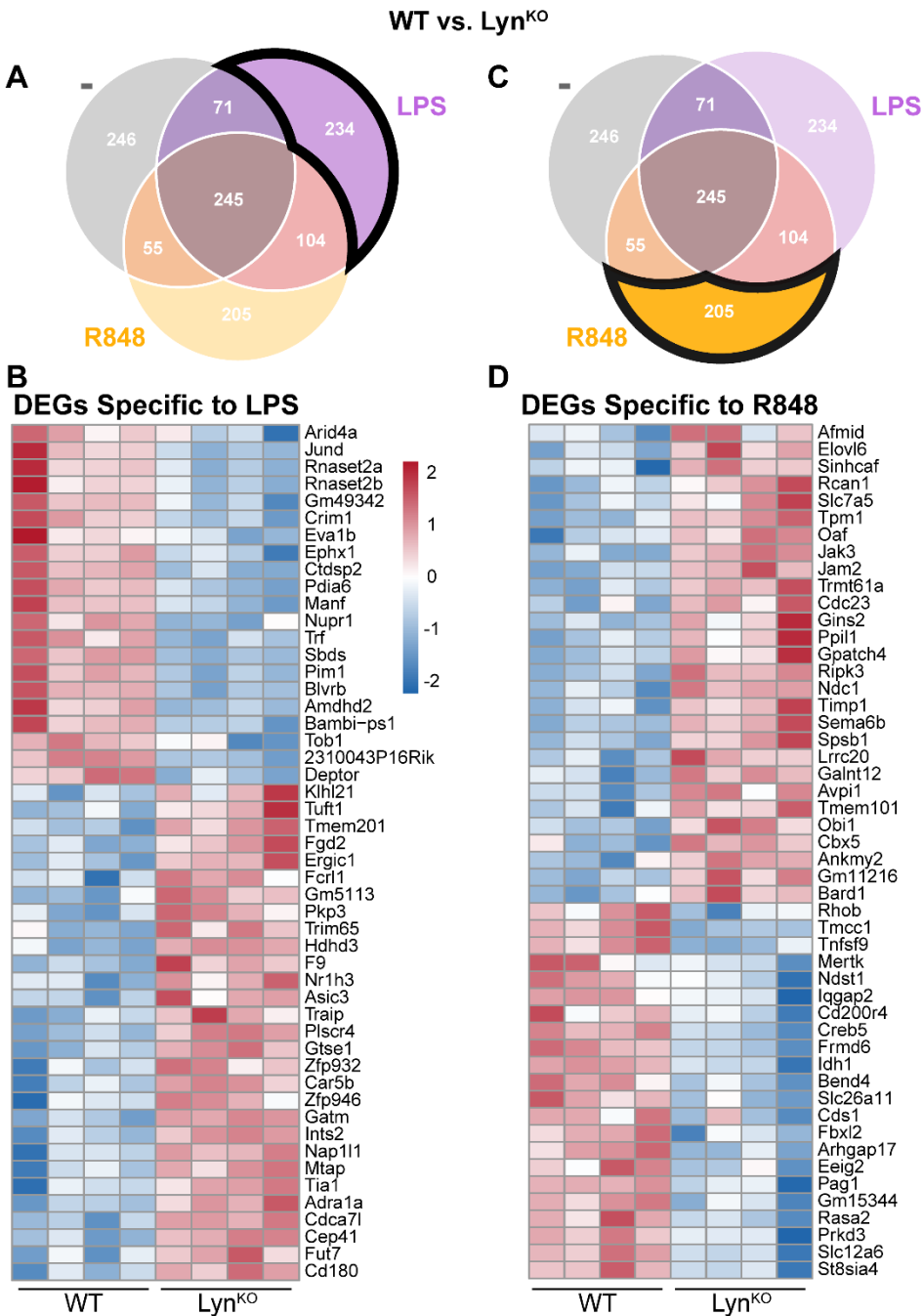


Figure 5. LPS- and R848-induced expression patterns are affected differentially by Lyn knockout in BMDMs. (A) Venn diagram highlighting LPS-specific DEGs in WT and Lyn^{KO} BMDMs. **(B)** Heat map showing the 50 highest-significance LPS-specific DEGs in WT and Lyn^{KO} BMDMs. **(C)** Venn diagram highlighting R848-specific DEGs in WT and Lyn^{KO} BMDMs. **(D)** Heat map showing the 50 highest-significance R848-specific DEGs in WT and Lyn^{KO} BMDMs. Heat maps and DEGs were compiled as described in Fig. 2.

Gene products such as *Jund* (an AP-1-family transcription factor), *Nupr1* (an autophagy suppressor), and *Pim1* (a Ser/Thr kinase that restricts cell growth) were uniquely downregulated, while *Traip* (an E3 ubiquitin ligase) and *Pkp3* (plakophilin, a component of desmosomes) were upregulated (**Fig. 5B**). In WT and Lyn^{KO} BMDMs, we identified 205 DEGs found only in R848-treated samples (**Fig. 5C**). Gene products such as *Tnfsf9* (4-1BBL, promoter of T-cell co-stimulation) and *Mertk* (receptor tyrosine kinase) were uniquely downregulated, while *Jak3* (tyrosine kinase mediating cytokine responses), *Jam2* (cellular-junction adhesion molecule), and *Timp1* (inhibitor of MMP activity) were upregulated (**Fig. 5D**). There were few LPS-specific DEGs in LynA^{KO} or LynB^{KO} BMDMs and WT, but both genotypes had decreased expression of *Serpinb9* (**Sup. Fig. 1C**). There were no remarkable R848-specific DEGs in the single-isoform knockouts.

Despite the presence of TLR-specific responses to Lyn deletion, no clear segregation of receptor-specific signaling pathways emerged, and most of the DEGs were not associated with canonical TLR signaling cascades, such as NF-kB-, MAPK-, or IRF-driven transcription. Nevertheless, we found significantly impaired induction of Erk and Akt phosphorylation in Lyn^{KO} BMDMs after treatment with LPS, with trending decreases in Jnk and Ikk phosphorylation (**Sup. Fig. 4A**). Similarly, R848-induced phosphorylation of Erk, Jnk, and Akt was reduced in Lyn^{KO} BMDMs, and Ikk phosphorylation was not impacted (**Sup. Fig. 4B**). These data suggest that Lyn expression is required for signal transduction downstream of both TLR4 and TLR7, and the absence of Lyn results in a broad attenuation of TLR-driven signaling rather than selective disruption of individual receptor-associated pathways.

To refine our transcriptome-wide analyses of DEGs in WT and Lyn^{KO} BMDMs, we used gene-set enrichment analysis (GSEA) to probe which cellular functions appear to be most perturbed by the loss of Lyn (**Sup. Fig. 5**). We found basal enrichment of E2F-targeted gene pathways (**Fig. 6A**) and mitotic-spindle-related gene pathways (**Fig. 6B**) in Lyn^{KO} BMDMs.

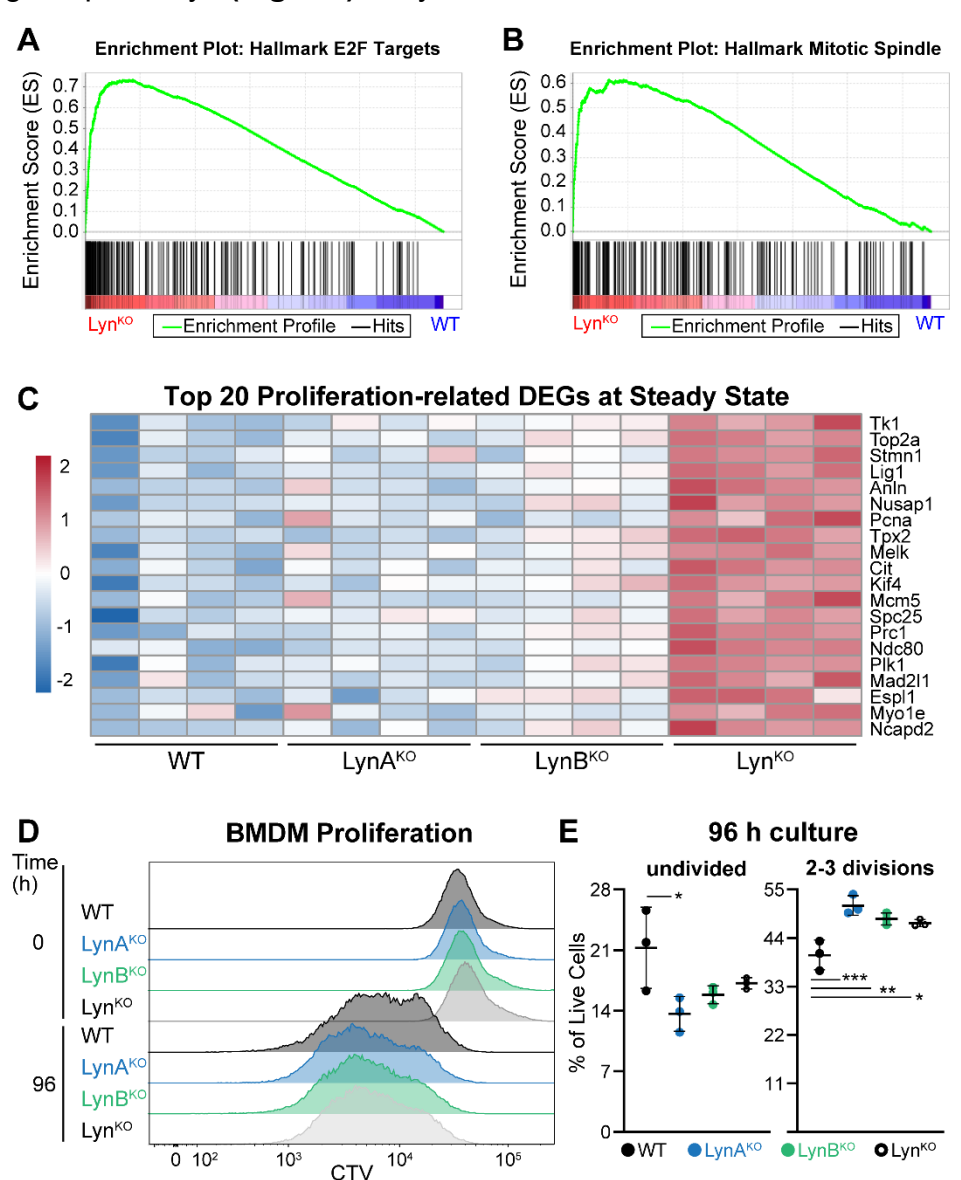


Figure 6. LynKO BMDMs have enhanced cell proliferation at steady state. (A,B) GSEA showing enrichment of (A) E2F-targeted and (B) mitotic-spindle-related genes in Lyn^{KO} BMDMs at steady state. (C) Heat map of the 20 highest-significance DEGs related to proliferation in WT and Lyn^{KO} BMDMs. Heat maps and DEGs were compiled as described in Fig. 2. (D) Representative flow-cytometry histograms showing CTV fluorescence in BMDMs immediately after dye loading or after 96 h culture in M-CSF-containing medium. (E) Quantification of parental and dividing cells after 96 h (n=3). The parent generation was identified by the CTV peak at t=0, and subsequent generations were identified using FlowJo software. Data are presented as mean ± standard deviation. Significance was assessed via two-way ANOVA with Tukey's multiple comparisons test. p values 0.01-0.03 *, 0.007 ***, 0.001 ***. There were no significant differences between non-annotated pairs. n=3 biological replicates derived from different mice.

As the E2F transcription factor and formation of a mitotic spindle are key components of cell proliferation⁶⁶, we searched the DEG pool for other pro-mitotic gene products. Indeed, we found that Lyn^{KO}, but not single-isoform knockout BMDMs, upregulate gene products promoting DNA synthesis, replication, and repair (e.g., *Tk1*, *Top2a*, *Lig1*, *Pcna*, *Mcm5*) and mitotic microtubule rearrangement (e.g., *Stmn1*, *Anln*, *Nusap1*, *Tpx2*, *Melk*, *Cit*, *Kif4*, *Spc25*, *Prc1*, *Ndc80*, *Plk1*, *Mad2l1*, *Espl1*, *Ncapd2*, **Fig. 6C**). To

test the functional consequences of these transcriptional changes, we measured proliferation of WT, LynA^{KO}, LynB^{KO}, and Lyn^{KO} BMDMs in culture. Consistent with previous findings with Lyn^{KO} BMDMs⁶⁷, we observed enhanced proliferation of Lyn^{KO} cells in culture, demonstrated by more dye dilution in Lyn^{KO} BMDMs than WT (**Fig. 6D**). Comparing parental and divided cells at 96 hours, we found that Lyn^{KO} BMDMs were significantly more likely to divide than WT (**Fig. 6E**). Interestingly, though the transcriptional profile of LynA^{KO} and LynB^{KO} BMDMs only trended toward an intermediate phenotype, these cells also exhibited a greater degree of proliferation than WT in culture. Since neither LynA nor LynB alone is sufficient to restrain cell proliferation, it is likely that a higher expression level of total Lyn protein must be maintained for this process than for other cellular functions.

GSEA also revealed TLR-induced transcriptional changes in Lyn^{KO} BMDMs that favor ECM formation. After either LPS **(Fig. 7A)** or R848 **(Fig. 7B)** treatment, Lyn^{KO} cells had enhanced expression of core matrisome genes, with many of these having a greater magnitude of differential expression than at steady state.

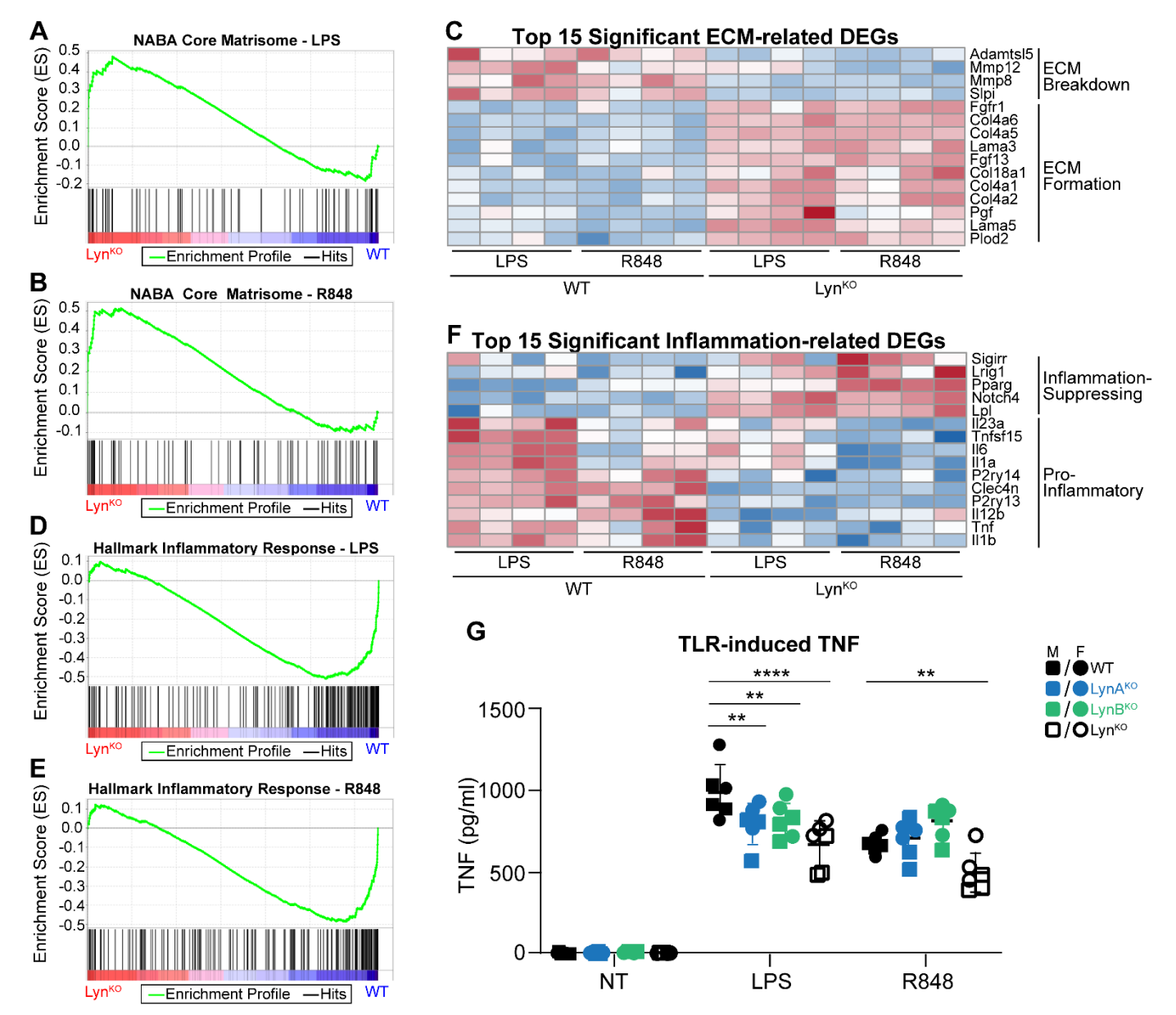


Figure 7. LynKO BMDMs have enhanced expression of genes driving ECM synthesis and impaired inflammatory cytokine production after TLR stimulation. (A,B) GSEA showing enrichment of core matrisome genes in Lyn^{KO} BMDMs relative to WT after (A) LPS or (B) R848 treatment. (C) Heat map of the 15 highest-significance DEGs related to ECM formation in WT and Lyn^{KO} BMDMs. (D,E) GSEA showing enrichment of inflammatory response genes in WT and Lyn^{KO} BMDMs after (D) LPS or (E) R848 treatment. (F) Heat map of the 15 highest-significance DEGs related to inflammatory response in WT and Lyn^{KO} BMDMs. Heat maps and DEGs were compiled as described in Fig. 2. (G) ELISA showing TNF production by WT, LynA^{KO}, LynB^{KO}, and total Lyn^{KO} BMDMs at steady state and after 24 h treatment with 2 ng/ml LPS or 20 ng/ml R848 (n=6). Data are presented as mean ± standard deviation. Significance was assessed via two-way ANOVA with Tukey's multiple comparisons test. p-value <0.05 *, <0.01 ***, <0.001 ****, <0.0001 ****, with all other pairwise comparisons lacking significant differences. Outlier analysis was performed using unbiased ROUT with Q=1%. n indicates the number of biological replicates, with cells from different individual mice. Squares indicate cells derived from male mice, and circles indicate cells derived from female mice.

Notably, genes that prompt the synthesis of ECM components and expansion of the ECM (e.g., *Col4a1*, *Col4a2*, *Col4a5*, *Col4a6*, *Lama3*, *Lama5*, *Fgfr1*, *Fgf13*, *Pgf*, *Plod2*) were upregulated in Lyn^{KO} cells, while those that facilitate ECM degradation (e.g., *Mmp8*, *Mmp12*, *Adamtsl5*, *Slpi*) were downregulated relative to WT (**Fig. 7C**). These data suggest that Lyn promotes ECM turnover, and defects in Lyn can lead to overgrowth of the ECM.

Lastly, GSEA more broadly confirmed the impairment of TLR-induced inflammatory responses by Lyn^{KO} BMDMs. Hallmark gene sets for inflammatory response, TNF signaling via NF-kB, IL-6/JAK/STAT3 signaling, and complement were all underexpressed in Lyn^{KO} cells after LPS (Fig. 7D) or R848 (Fig. **7E)** treatment. Lyn^{KO} BMDMs had decreased induction of genes driving inflammatory signaling (e.g., P2ry13, P2ry14, Clec4n) and cytokine production (e.g., II1a, II1b, II6, II12b, II23a, Tnf, Tnfsf15) in tandem with failure to downregulate expression of immunosuppressive gene products (e.g., Lpl, Lrig1, Notch4, Pparg, Sigirr, Fig. 7F). qRT-PCR analyses revealed significantly decreased transcription of II1b and II6 in LynKO BMDMs up to 8 hours after treatment with LPS (Sup. Fig. 6A) or R848 (Sup. Fig. 6B). Tnf induction peaked at earlier time points, and R848-treated LynKO cells had significantly reduced transcription of *Tnf* after 4-hours, whereas LPS-treated Lyn^{KO} cells showed only trending decreases in *Tnf* transcription. To ensure that differences in mRNA expression were translated to the protein level, we analyzed TLR-induced TNF secretion by BMDMs after 24 hours of treatment with LPS or R848. Quantifying TNF secretion via ELISA, we found that Lyn^{KO} BMDMs had diminished TLR responses, secreting 2-fold less TNF protein than WT cells after treatment with LPS or R848 (Fig. 7G). Although there is no isoform-specific contribution to TNF production, TLR4 and TLR7 require different total amounts of Lyn expression to function at a WT level— LPS-treated LynAKO and LynBKO BMDMs had impaired TNF secretion, albeit to a lesser degree than Lyn^{KO}, whereas the single-isoform Lyn knockouts had no defect in R848-induced TNF production. We therefore conclude that TLR4 requires higher levels of Lyn expression than TLR7 to maintain WT-like levels of signaling.

Discussion

In this study we report that macrophage expression of either LynA or LynB is sufficient to promote TLR sensitivity, expression of matrix remodeling machinery, and inflammatory signaling and that complete loss of Lyn disrupts these essential macrophage functions. Both at steady state and after treatment with TLR4 or TLR7 agonist, the expression of either Lvn isoform restores most of the widespread transcriptomic changes seen in Lyn-deficient macrophages. At steady state, Lyn restricts the expression of genes driving DNA synthesis and replication, mitosis, and cell growth, which leads to inhibition of macrophage proliferation in culture. Interestingly, despite restoring normal expression of proliferation-related genes, single-isoform expression of Lyn is ineffective at preventing macrophage hyperproliferation, suggesting that a full complement of Lyn expression is necessary for direct signaling beyond simple transcriptomic regulation. Lyn also exerts transcriptional control over ECM remodeling by driving the expression of genes that promote ECM degradation and restricting genes that direct the synthesis of structural proteins and ECM components, both at steady state and after TLR activation, Lastly, Lyn plays an important role in balancing inflammatory and immunosuppressive signaling pathways downstream of TLRs. Single-isoform expression of Lyn is sufficient for TLR7-driven cytokine production, while TLR4-induced TNF production appears to require full complement of both LynA and LynB. Regardless, there does not appear to be any Lyn isoform specificity in TLR4 or TLR7-induced cytokine production. Notably, Lyn deficiency does not affect TLR mRNA or protein expression in macrophages. These findings indicate that expression of either Lyn isoform is sufficient to maintain most of the canonical TLR responses and suppress dysregulated ECM formation in macrophages, although inadeguate expression of total Lyn may be insufficient to fully restore proliferation control.

Transcriptomic enrichment of E2F targets and mitotic spindle components in Lyn^{KO} cells supports a model in which Lyn deficiency relieves molecular checks on cell-cycle progression, consistent with patterns in DCs⁶⁷, myeloid progenitors⁶⁸, and patrolling monocytes⁶⁹. The observation that both LynA^{KO} and LynB^{KO} BMDMs proliferate more than WT, despite lacking robust transcriptional activation of the same cell-cycle programs, suggests that Lyn may restrain proliferation in a dose-dependent rather than isoform-specific manner. Furthermore, the marginal increase in proliferation-associated gene transcription that is seen with a single-isoform deficiency of Lyn may be sufficient to drive a hyperproliferative response to M-CSF. These findings raise the possibility that Lyn contributes to the maintenance of macrophage quiescence under homeostatic conditions and that loss of Lyn expression tips the balance toward expansion, even in the absence of strong mitogenic cues. Given the importance of controlled

macrophage turnover in resolving inflammation and maintaining tissue integrity⁷⁰, Lyn may serve as a key regulator of macrophage population dynamics in both steady-state and inflammatory settings.

Our study also suggests that Lyn plays an underappreciated role in controlling ECM dynamics in macrophages. Lyn^{KO} BMDMs have increased expression of genes encoding collagen IV, laminins, and ECM cross-linking enzymes and reduced expression of genes encoding matrix-degrading metalloproteases such as MMP8 and MMP12. This shift toward an ECM-producing/preserving phenotype could impair immune-cell trafficking and tissue remodeling, contributing to pathological fibrosis. These transcriptomic findings are consistent with our previous work showing increased fibrosis in kidneys from aged Lyn^{KO} mice³⁴. Conversely, a macrophage phenotype that promotes ECM synthesis and limits ECM degradation may be beneficial in suppressing cancer growth and metastasis. The ECM plays a complex role in cancer progression, where increased matrix breakdown can promote cancer-cell growth and metastasis, yet a thickened ECM can impair responsiveness to chemotherapy⁷¹. On the other hand, a collagen-rich ECM might suppress cancer growth by limiting the availability of oxygen and nutrients⁷². Lyn expression in macrophages within the tumor microenvironment promotes cancer-cell growth, and Lyn-deficient macrophages delay the progression of chronic lymphocytic leukemia and prolong patient survival⁷³. Furthermore, Lyn-deficient stromal fibroblasts reduce cancer growth by acquiring a myofibroblastic phenotype, characterized by increased ECM formation and reduced production of inflammatory cytokines⁷⁴. Thus, treatments targeting Lyn-mediated pathways in macrophages within tumors may prove beneficial in reducing cancer growth and metastasis by reducing ECM remodeling and limiting inflammation.

The impaired inflammatory response of Lyn-deficient macrophages underscores the importance of Lynas a positive driver of immune signaling. While several studies have shown that Lyn inhibits TLR signaling in classical DCs and B cells^{35-37,39}, our findings align with reports indicating that Lyn is required for optimal TLR-induced cytokine production in macrophages^{46,47,49-51}. A few studies provide mechanistic hints into the TLR-promoting function of Lyn. In mast cells, Lyn drives TLR4-induced transcription of inflammatory cytokines, such as TNF, by associates with TRAF6, leading to TRAF6 polyubiquitination and TAK1 phosphorylation, driving IKK and MAPK activation⁵¹. Lyn^{KO} mast cells have reduced TLR4-induced phosphorylation of NFkB, Erk, Jnk, and p38⁵¹. We also found impaired TLR-induced phosphorylation of Erk and Jnk in Lyn^{KO} cells, indicating Lyn functions upstream of NF-κB and MAPK pathways, perhaps by facilitating TRAF6 activation. Lyn functions similarly in macrophages⁵⁰ and pDCs³⁹, promoting TLR2- and TLR7-induced NF-kB activation and cytokine production, an effect that requires functional kinase activity. Interestingly, Lyn-mediated PI3K phosphorylation, resulting in Akt phosphorylation and culminating with NF-kB activation, may also explain how Lyn facilitates TLR signaling in macrophages^{49,50}. Concordantly, we saw impaired P-Akt induction in Lyn^{KO} BMDMs after TLR4 and TLR7 stimulation. Of note, Lyn may also mediate JAK/STAT signaling and responses to cytokines themselves, such as IL-6⁷⁵. Thus, it may be difficult to uncouple differences from autocrine cytokine signaling with those from direct TLR-activation, especially at longer time points. Our GSEA did suggest impaired IL6/JAK/STAT signaling in TLR-treated Lyn^{KO} BMDMs, however, using a 2-hour treatment, our RNA sequencing data likely reflect directly TLR-induced signaling differences. One limitation of our study is using M-CSF-derived macrophages, where CSFR-driven signaling may influence the interpretation of TLR-driven responses. Given that Lyn^{KO} cells are hyperresponsive to M-CSF⁶⁷, it is worth considering that negative feedback loops may be induced by chronic, hyperactive CSFR activation and could exert an inhibitory influence on TLR signaling.

It is not clear why the impact of Lyn on TLR signaling responses differs in DCs. Stimulation through several different TLRs drives increased cytokine production by Lyn^{KO} splenic DCs^{37-39,42,43}. Lyn has a specific role in inhibiting Type-I IFN production through phosphorylating IRFs, leading to polyubiquitination and degradation⁴³. This is dependent on the kinase activity of Lyn and is regulated by Csk⁴². The mechanism by which Lyn affects other TLR signaling pathways is less well understood, but Lyn can act downstream of MyD88³⁷ and CARD9³⁸ to inhibit NF-κB and MAPK activation in DCs. This inhibitory role of Lyn is also dependent on Hck and Fgr.³⁸ This finding provides one possible explanation

for the differing roles of Lyn in macrophages/pDCs and cDCs. Macrophages and pDCs have much lower expression of Hck than cDCs³⁹ and may not be equipped to recruit other SFKs as compensatory drivers of TLR signaling. Thus a loss of Lyn in macrophages may function similarly to a loss of Lyn and Hck in cDCs. Indeed, Lyn/Hck/Fgr triple knockout DCs produce fewer cytokines than WT following TLR stimulation³⁸, similarly to Lyn^{KO} macrophages. Furthermore, overexpressing Hck in Lyn-deficient macrophages can lead to a robust increase in TLR4-induced TNF and IL-6.⁴⁸ Other possible explanations of opposite Lyn function in these two cell types may relate to differential expression of binding partners, other negative regulators (e.g., the inositol phosphatase SHIP1), or TLR adapter proteins.

Nevertheless, these findings suggest that the inflammatory phenotype observed in Lyn^{KO} mice may be driven predominantly by immune cells not of the macrophage lineage or by cell-extrinsic effects on macrophages in vivo. For instance, macrophage-related pathologies in Lyn^{KO} mice, such as glomerulonephritis, may arise from the exacerbated inflammatory environment created by dysregulated, Lyndeficient DCs^{37,38} and mature B cells^{35,36} rather than innate inflammatory signaling by Lyn^{KO} macrophages.

We show that either LynA or LynB can promote TLR-induced cytokine production in macrophages. Partially impaired TLR4-driven TNF production in macrophages with single-isoform Lyn expression likely results from reduced levels of total Lyn in these cells, indicating a dose-dependent rather than isoform-specific requirement for signaling. This is supported by a previous observation that even a partial loss of Lyn can promote B-cell dysregulation and autoimmunity⁷⁶. Defining how Lyn modulates signaling thresholds across different myeloid subsets and downstream of different receptors will be a critical step in resolving these apparent contradictions and elucidating how Lyn orchestrates balanced immune responses.

Our findings support a model in which Lyn acts as a positive regulator of macrophage activation down-stream of TLRs, while simultaneously serving as a brake on pathological proliferation and ECM accumulation. These dual roles may reflect a broader homeostatic function for Lyn in tuning macrophage responses to inflammatory stimuli, enabling robust immune activation while limiting myeloid-cell expansion and tissue fibrosis. Given that expression of either LynA or LynB alone can restore many macrophage functions to WT-like levels, therapies aimed at boosting total Lyn expression or function could offer greater benefit than isoform-specific modulation. Future studies dissecting the mechanistic contributions of LynA and LynB to specific signaling nodes — particularly their interactions with adaptor proteins and downstream kinases — will be essential for translating these insights into therapeutic approaches.

Authorship

AJL: Conceptualization, Methodology, Investigation, Data curation, Formal analysis, Visualization, Writing – original draft, Writing – review & editing, Funding acquisition. JTG: Methodology, Investigation, Formal analysis, Writing – review & editing, Funding acquisition. YX: Validation, Data curation, Writing – review & editing. TSF: Conceptualization, Methodology, Visualization, Writing – review & editing, Supervision, Project administration, Funding acquisition.

Acknowledgements

We thank Dr. Tyler Bold, Dr. Natalia Calixto Mancipe, and Charlie Roll for contributions to analysis and presentation of RNA sequencing data. Thanks also to Drs. Bryce Binstadt, Vaiva Vezys, and Li-Na Wei for feedback on project goals and presentation.

Funding

This work was supported by National Institutes of Health awards R03Al130978, R01AR073966, R01AR084525, and R56AR084525 (all TSF); R01Al165553 (JWW); and Rheumatology Research Foundation Innovative Research Award 889928 (TSF). Training support was provided by National Institutes of Health awards T32HL007741 (AJL) and T32CA009138 (JTG), University of Minnesota

Dinnaken Fellowship (AJL), and American Cancer Society–Kirby Foundation Postdoctoral Fellowship PF-21-068-01-LIB (JTG). Research reported in this publication was also supported by the National Institute of General Medical Sciences of the National Institutes of Health under Award Number T32GM156735 (AJL). The content is solely the responsibility of the authors and does not necessarily represent the official views of the National Institutes of Health.

Data Availability

RNA sequencing data have been deposited in the NCBI Gene Expression Omnibus (GEO) under accession number x. The remaining data analyzed in the above study are available from the corresponding authors upon request.

References

- 1. Campuzano, A.; Castro-Lopez, N.; Martinez, A. J.; Olszewski, M. A.; Ganguly, A.; Leopold Wager, C.; Hung, C.-Y.; Wormley, F. L. CARD9 Is Required for Classical Macrophage Activation and the Induction of Protective Immunity against Pulmonary Cryptococcosis. *mBio* **2020**, *11* (1), e03005-19. DOI: 10.1128/mBio.03005-19
- 2. Iwata, Y.; Boström, E. A.; Menke, J.; Rabacal, W. A.; Morel, L.; Wada, T.; Kelley, V. R. Aberrant Macrophages Mediate Defective Kidney Repair That Triggers Nephritis in Lupus-Susceptible Mice. *J Immunol* **2012**, *188* (9), 4568–4580.
- Scapini, P.; Hu, Y.; Chu, C.-L.; Migone, T.-S.; DeFranco, A. L.; Cassatella, M. A.; Lowell, C. A. Myeloid Cells, BAFF, and IFN-γ Establish an Inflammatory Loop That Exacerbates Autoimmunity in Lyn-Deficient Mice. *J Exp Med* 2010, 207 (8), 1757–1773.
- Morse, C.; Tabib, T.; Sembrat, J.; Buschur, K. L.; Bittar, H. T.; Valenzi, E.; Jiang, Y.; Kass, D. J.; Gibson, K.; Chen, W.; Mora, A.; Benos, P. V.; Rojas, M.; Lafyatis, R. Proliferating SPP1/MERTK-Expressing Macrophages in Idiopathic Pulmonary Fibrosis. *Eur Respir J* 2019, 54 (2), 1802441. DOI: 10.1183/13993003.02441-2018
- Gibbons, M. A.; MacKinnon, A. C.; Ramachandran, P.; Dhaliwal, K.; Duffin, R.; Phythian-Adams, A. T.; van Rooijen, N.; Haslett, C.; Howie, S. E.; Simpson, A. J.; Hirani, N.; Gauldie, J.; Iredale, J. P.; Sethi, T.; Forbes, S. J. Ly6Chi Monocytes Direct Alternatively Activated Profibrotic Macrophage Regulation of Lung Fibrosis. *Am J Respir Crit Care Med* 2011, 184 (5), 569–581.
- 6. Shen, B.; Liu, X.; Fan, Y.; Qiu, J. Macrophages Regulate Renal Fibrosis through Modulating TGFβ Superfamily Signaling. *Inflammation* **2014**, *37* (6), 2076–2084.
- 7. Jalil, A. R.; Andrechak, J. C.; Discher, D. E. Macrophage Checkpoint Blockade: Results from Initial Clinical Trials, Binding Analyses, and CD47-SIRPα Structure-Function. *Antib Ther* **2020**, 3 (2), 80–94.
- 8. Zhang, Y.; Cheng, S.; Zhang, M.; Zhen, L.; Pang, D.; Zhang, Q.; Li, Z. High-Infiltration of Tumor-Associated Macrophages Predicts Unfavorable Clinical Outcome for Node-Negative Breast Cancer. *PLoS One* **2013**, *8* (9), e76147. DOI: 10.1371/journal.pone.0076147
- 9. Barkal, A. A.; Brewer, R. E.; Markovic, M.; Kowarsky, M.; Barkal, S. A.; Zaro, B. W.; Krishnan, V.; Hatakeyama, J.; Dorigo, O.; Barkal, L. J.; Weissman, I. L. CD24 Signalling through Macrophage Siglec-10 Is a Target for Cancer Immunotherapy. *Nature* **2019**, *572* (7769), 392–396.
- 10. Lin, B.; Dutta, B.; Fraser, I. D. C. Systematic Investigation of Multi-TLR Sensing Identifies Regulators of Sustained Gene Activation in Macrophages. *Cell Syst* **2017**, *5* (1), 25-37.e3. DOI: 10.1016/j.cels.2017.06.014
- 11. Barton, G. M.; Kagan, J. C.; Medzhitov, R. Intracellular Localization of Toll-like Receptor 9 Prevents Recognition of Self DNA but Facilitates Access to Viral DNA. *Nat Immunol* **2006**, *7* (1), 49–56.
- Forsbach, A.; Nemorin, J.-G.; Montino, C.; Müller, C.; Samulowitz, U.; Vicari, A. P.; Jurk, M.; Mutwiri, G. K.; Krieg, A. M.; Lipford, G. B.; Vollmer, J. Identification of RNA Sequence Motifs Stimulating Sequence-Specific TLR8-Dependent Immune Responses. *J Immunol* 2008, 180 (6), 3729–3738.

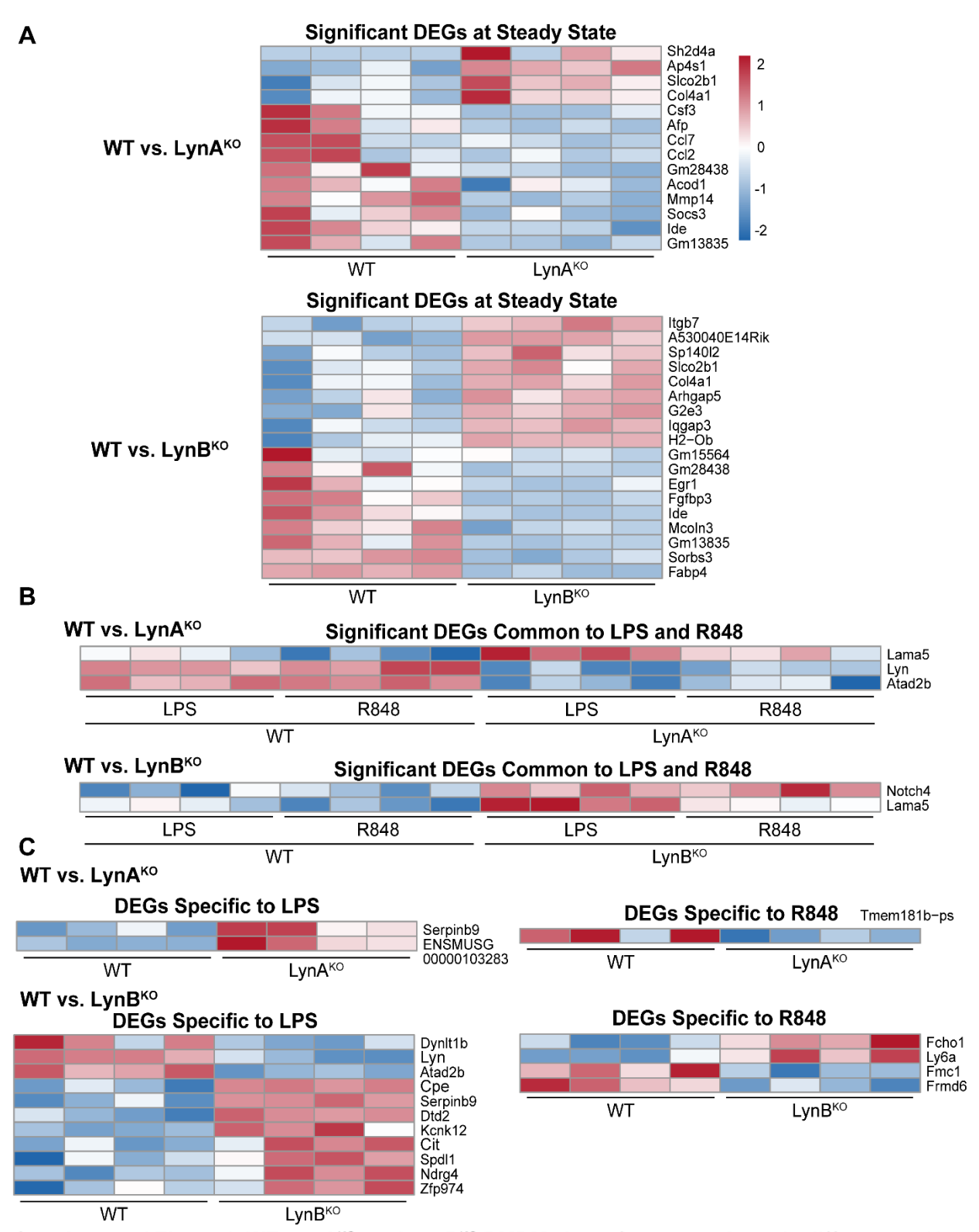
- 13. Latz, E.; Schoenemeyer, A.; Visintin, A.; Fitzgerald, K. A.; Monks, B. G.; Knetter, C. F.; Lien, E.; Nilsen, N. J.; Espevik, T.; Golenbock, D. T. TLR9 Signals after Translocating from the ER to CpG DNA in the Lysosome. *Nat Immunol* **2004**, *5* (2), 190–198.
- 14. Park, J. S.; Svetkauskaite, D.; He, Q.; Kim, J.-Y.; Strassheim, D.; Ishizaka, A.; Abraham, E. Involvement of Toll-like Receptors 2 and 4 in Cellular Activation by High Mobility Group Box 1 Protein. *J Biol Chem* **2004**, *279* (9), 7370–7377.
- 15. Fang, H.; Wu, Y.; Huang, X.; Wang, W.; Ang, B.; Cao, X.; Wan, T. Toll-like Receptor 4 (TLR4) Is Essential for Hsp70-like Protein 1 (HSP70L1) to Activate Dendritic Cells and Induce Th1 Response *. Journal of Biological Chemistry 2011, 286 (35), 30393–30400.
- 16. Kawai, T.; Akira, S. Toll-like Receptors and Their Crosstalk with Other Innate Receptors in Infection and Immunity. *Immunity* **2011**, *34* (5), 637–650.
- 17. Li, X.; Jiang, S.; Tapping, R. I. Toll-like Receptor Signaling in Cell Proliferation and Survival. *Cytokine* **2010**, *49* (1), 1–9.
- 18. Lim, E.-J.; Lee, S.-H.; Lee, J.-G.; Chin, B.-R.; Bae, Y.-S.; Kim, J.-R.; Lee, C.-H.; Baek, S.-H. Activation of Toll-like Receptor-9 Induces Matrix Metalloproteinase-9 Expression through Akt and Tumor Necrosis Factor-Alpha Signaling. *FEBS Lett* **2006**, *580* (18), 4533–4538.
- 19. Bhattacharyya, S.; Kelley, K.; Melichian, D. S.; Tamaki, Z.; Fang, F.; Su, Y.; Feng, G.; Pope, R. M.; Budinger, G. R. S.; Mutlu, G. M.; Lafyatis, R.; Radstake, T.; Feghali-Bostwick, C.; Varga, J. Toll-Like Receptor 4 Signaling Augments Transforming Growth Factor-β Responses: A Novel Mechanism for Maintaining and Amplifying Fibrosis in Scleroderma. *The American Journal of Pathology* **2013**, *182* (1), 192–205.
- 20. Akira, S.; Takeda, K. Toll-like Receptor Signalling. Nat Rev Immunol 2004, 4 (7), 499-511.
- 21. Duan, T.; Du, Y.; Xing, C.; Wang, H. Y.; Wang, R.-F. Toll-Like Receptor Signaling and Its Role in Cell-Mediated Immunity. *Front. Immunol.* **2022**, *13*. DOI: 10.3389/fimmu.2022.812774
- 22. Wang, C.; Khatun, M. S.; Ellsworth, C. R.; Chen, Z.; Islamuddin, M.; Nisperuza Vidal, A. K.; Afaque Alam, M.; Liu, S.; Mccombs, J. E.; Maness, N. J.; Blair, R. V.; Kolls, J. K.; Qin, X. Deficiency of Tlr7 and Irf7 in Mice Increases the Severity of COVID-19 through the Reduced Interferon Production. *Commun Biol* **2024**, *7* (1), 1162. DOI: 10.1038/s42003-024-06872-5
- 23. Liu, W.; Ouyang, X.; Yang, J.; Liu, J.; Li, Q.; Gu, Y.; Fukata, M.; Lin, T.; He, J. C.; Abreu, M.; Unkeless, J. C.; Mayer, L.; Xiong, H. AP-1 Activated by Toll-like Receptors Regulates Expression of IL-23 P19*. *Journal of Biological Chemistry* **2009**, *284* (36), 24006–24016.
- 24. Lee, Y.-S.; Lan Tran, H. T.; Van Ta, Q. Regulation of Expression of Matrix Metalloproteinase-9 by JNK in Raw 264.7 Cells: Presence of Inhibitory Factor(s) Suppressing MMP-9 Induction in Serum and Conditioned Media. *Exp Mol Med* **2009**, *41* (4), 259–268.
- 25. Park, J. M.; Greten, F. R.; Wong, A.; Westrick, R. J.; Arthur, J. S. C.; Otsu, K.; Hoffmann, A.; Montminy, M.; Karin, M. Signaling Pathways and Genes That Inhibit Pathogen-Induced Macrophage Apoptosis— CREB and NF-κB as Key Regulators. *Immunity* **2005**, *23* (3), 319–329.
- 26. Sanin, D. E.; Prendergast, C. T.; Mountford, A. P. IL-10 Production in Macrophages Is Regulated by a TLR-Driven CREB-Mediated Mechanism That Is Linked to Genes Involved in Cell Metabolism. *J Immunol* **2015**, *195* (3), 1218–1232.
- 27. Aziz, N.; Kang, Y.-G.; Kim, Y.-J.; Park, W.-S.; Jeong, D.; Lee, J.; Kim, D.; Cho, J. Y. Regulation of 8-Hydroxydaidzein in IRF3-Mediated Gene Expression in LPS-Stimulated Murine Macrophages. *Biomolecules* **2020**, *10* (2), 238. DOI: 10.3390/biom10020238
- 28. Lazear, H. M.; Lancaster, A.; Wilkins, C.; Suthar, M. S.; Huang, A.; Vick, S. C.; Clepper, L.; Thackray, L.; Brassil, M. M.; Virgin, H. W.; Nikolich-Zugich, J.; Moses, A. V.; Michael Gale, J.; Früh, K.; Diamond, M. S. IRF-3, IRF-5, and IRF-7 Coordinately Regulate the Type I IFN Response in Myeloid Dendritic Cells Downstream of MAVS Signaling. *PLoS Pathogens* 2013, 9 (1), e1003118. DOI: 10.1371/journal.ppat.1003118
- 29. Brian, B. F., IV; Freedman, T. S. The Src-Family Kinase Lyn in Immunoreceptor Signaling. *Endocrinology* **2021**, *162* (10), bqab152. DOI: 10.1210/endocr/bqab152

- 30. L'Estrange-Stranieri, E.; Gottschalk, T. A.; Wright, M. D.; Hibbs, M. L. The Dualistic Role of Lyn Tyrosine Kinase in Immune Cell Signaling: Implications for Systemic Lupus Erythematosus. *Frontiers in Immunology* **2024**, *15*, 1395427. DOI: 10.3389/fimmu.2024.1395427
- 31. Scapini, P.; Lamagna, C.; Hu, Y.; Lee, K.; Tang, Q.; DeFranco, A. L.; Lowell, C. A. B Cell-Derived IL-10 Suppresses Inflammatory Disease in Lyn-Deficient Mice. *Proceedings of the National Academy of Sciences* **2011**, *108* (41), E823–E832. DOI: 10.1073/pnas.1107913108
- 32. Hibbs, M. L.; Tarlinton, D. M.; Armes, J.; Grail, D.; Hodgson, G.; Maglitto, R.; Stacker, S. A.; Dunn, A. R. Multiple Defects in the Immune System of Lyn-Deficient Mice, Culminating in Autoimmune Disease. *Cell* **1995**, *83* (2), 301–311.
- 33. Chan, V. W.; Meng, F.; Soriano, P.; DeFranco, A. L.; Lowell, C. A. Characterization of the B Lymphocyte Populations in Lyn-Deficient Mice and the Role of Lyn in Signal Initiation and down-Regulation. *Immunity* **1997**, *7* (1), 69–81.
- 34. Brian, B. F., IV; Sauer, M. L.; Greene, J. T.; Senevirathne, S. E.; Lindstedt, A. J.; Funk, O. L.; Ruis, B. L.; Ramirez, L. A.; Auger, J. L.; Swanson, W. L.; Nunez, M. G.; Moriarity, B. S.; Lowell, C. A.; Binstadt, B. A.; Freedman, T. S. A Dominant Function of LynB Kinase in Preventing Autoimmunity. *Science Advances* **2022**, *8* (16), eabj5227. DOI: 10.1126/sciadv.abj5227
- 35. Tsantikos, E.; Oracki, S. A.; Quilici, C.; Anderson, G. P.; Tarlinton, D. M.; Hibbs, M. L. Autoimmune Disease in Lyn-Deficient Mice Is Dependent on an Inflammatory Environment Established by IL-6. *J Immunol* **2010**, *184* (3), 1348–1360.
- 36. Lamagna, C.; Hu, Y.; DeFranco, A. L.; Lowell, C. A. B Cell–Specific Loss of Lyn Kinase Leads to Autoimmunity. *The Journal of Immunology* **2014**, *192* (3), 919–928.
- 37. Lamagna, C.; Scapini, P.; van Ziffle, J. A.; DeFranco, A. L.; Lowell, C. A. Hyperactivated MyD88 Signaling in Dendritic Cells, through Specific Deletion of Lyn Kinase, Causes Severe Autoimmunity and Inflammation. *Proceedings of the National Academy of Sciences* **2013**, *110* (35), E3311–E3320. DOI: 10.1073/pnas.1300617110
- 38. Ma, J.; Abram, C. L.; Hu, Y.; Lowell, C. A. CARD9 Mediates Dendritic Cell-Induced Development of Lyn-Deficiency–Associated Autoimmune and Inflammatory Diseases. *Sci Signal* **2019**, *12* (602), eaao3829. DOI: 10.1126/scisignal.aao3829
- 39. Dallari, S.; Macal, M.; Loureiro, M. E.; Jo, Y.; Swanson, L.; Hesser, C.; Ghosh, P.; Zuniga, E. I. Src Family Kinases Fyn and Lyn Are Constitutively Activated and Mediate Plasmacytoid Dendritic Cell Responses. *Nat Commun* **2017**, *8* (1), 14830. DOI: 10.1038/ncomms14830
- 40. Keck, S.; Freudenberg, M.; Huber, M. Activation of Murine Macrophages via TLR2 and TLR4 Is Negatively Regulated by a Lyn/Pl3K Module and Promoted by SHIP1. *The Journal of Immunology* **2010**, *184* (10), 5809–5818.
- 41. Borzęcka-Solarz, K.; Dembińska, J.; Hromada-Judycka, A.; Traczyk, G.; Ciesielska, A.; Ziemlińska, E.; Świątkowska, A.; Kwiatkowska, K. Association of Lyn Kinase with Membrane Rafts Determines Its Negative Influence on LPS-Induced Signaling. *Mol Biol Cell* **2017**, *28* (8), 1147–1159.
- 42. Tawaratsumida, K.; Redecke, V.; Wu, R.; Kuriakose, J.; Bouchard, J. J.; Mittag, T.; Lohman, B. K.; Mishra, A.; High, A. A.; Häcker, H. A Phospho-Tyrosine–Based Signaling Module Using SPOP, CSK, and LYN Controls TLR-Induced IRF Activity. *Science Advances* **2022**, *8* (27), eabq0084. DOI: 10.1126/sciadv.abq0084
- 43. Ban, T.; Sato, G. R.; Nishiyama, A.; Akiyama, A.; Takasuna, M.; Umehara, M.; Suzuki, S.; Ichino, M.; Matsunaga, S.; Kimura, A.; Kimura, Y.; Yanai, H.; Miyashita, S.; Kuromitsu, J.; Tsukahara, K.; Yoshimatsu, K.; Endo, I.; Yamamoto, T.; Hirano, H.; Ryo, A.; Taniguchi, T.; Tamura, T. Lyn Kinase Suppresses the Transcriptional Activity of IRF5 in the TLR-MyD88 Pathway to Restrain the Development of Autoimmunity. *Immunity* **2016**, *45* (2), 319–332.
- 44. Hibbs, M. L.; Harder, K. W.; Armes, J.; Kountouri, N.; Quilici, C.; Casagranda, F.; Dunn, A. R.; Tarlinton, D. M. Sustained Activation of Lyn Tyrosine Kinase In Vivo Leads to Autoimmunity. *J Exp Med* **2002**, *196* (12), 1593–1604.
- 45. Chen, W.; Hong, S.-H.; Jenks, S. A.; Anam, F. A.; Tipton, C. M.; Woodruff, M. C.; Hom, J. R.; Cashman, K. S.; Faliti, C. E.; Wang, X.; Kyu, S.; Wei, C.; Scharer, C. D.; Mi, T.; Hicks, S.;

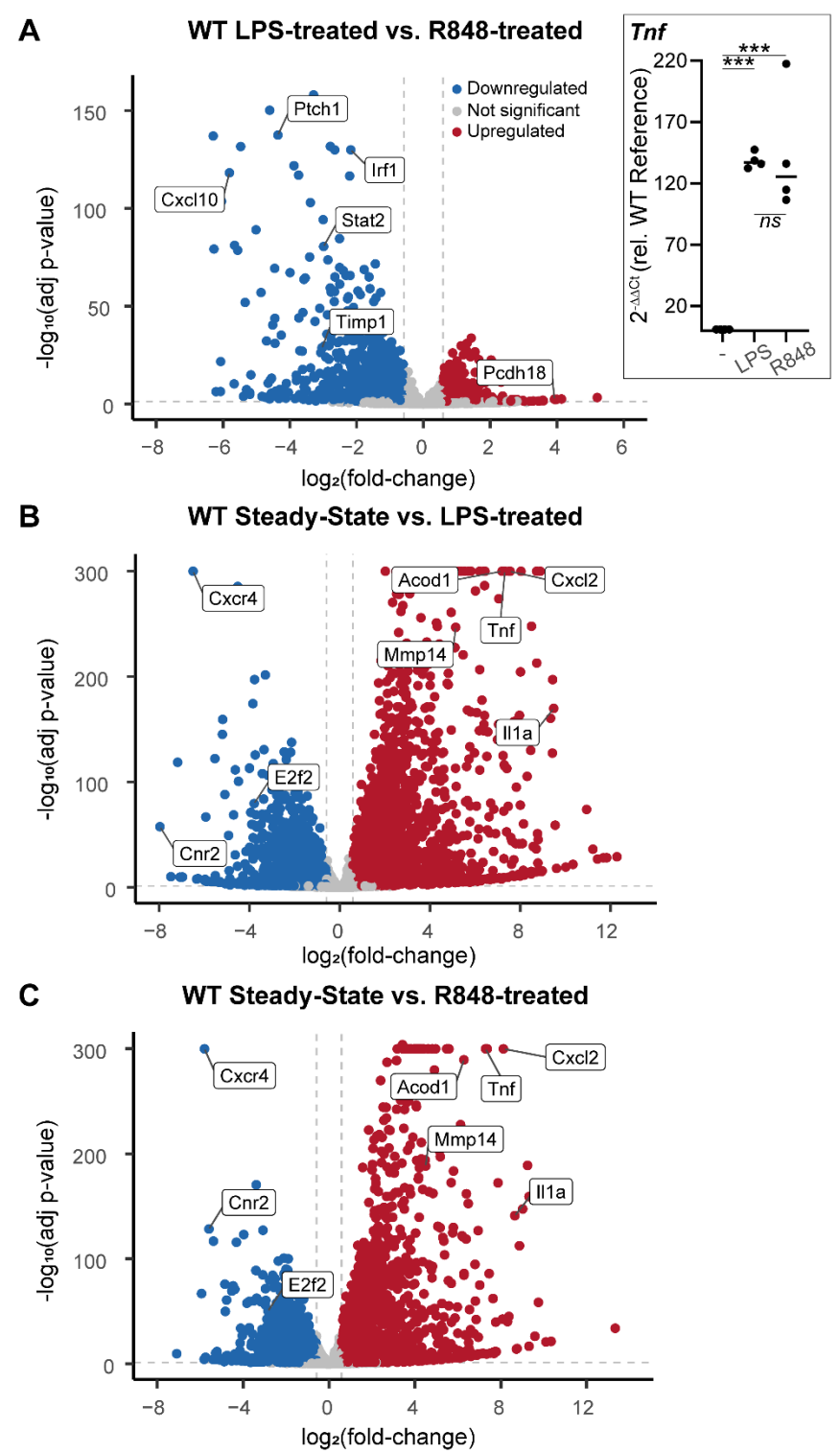
- Hartson, L.; Nguyen, D. C.; Khosroshahi, A.; Lee, S.; Wang, Y.; Bugrovsky, R.; Ishii, Y.; Lee, F. E.-H.; Sanz, I. Distinct Transcriptomes and Autocrine Cytokines Underpin Maturation and Survival of Antibody-Secreting Cells in Systemic Lupus Erythematosus. *Nat Commun* **2024**, 15, 1899. DOI: 10.1038/s41467-024-46053-w
- 46. Shio, M. T.; Eisenbarth, S. C.; Savaria, M.; Vinet, A. F.; Bellemare, M.-J.; Harder, K. W.; Sutterwala, F. S.; Bohle, D. S.; Descoteaux, A.; Flavell, R. A.; Olivier, M. Malarial Hemozoin Activates the NLRP3 Inflammasome through Lyn and Syk Kinases. *PLOS Pathogens* **2009**, *5* (8), e1000559. DOI: 10.1371/journal.ppat.1000559
- 47. Lim, Y. J.; Koo, J. E.; Hong, E.-H.; Park, Z.-Y.; Lim, K.-M.; Bae, O.-N.; Lee, J. Y. A Src-Family-Tyrosine Kinase, Lyn, Is Required for Efficient IFN-β Expression in Pattern Recognition Receptor, RIG-I, Signal Pathway by Interacting with IPS-1. *Cytokine* **2015**, *72* (1), 63–70.
- 48. Smolinska, M. J.; Page, T. H.; Urbaniak, A. M.; Mutch, B. E.; Horwood, N. J. Hck Tyrosine Kinase Regulates TLR4-Induced TNF and IL-6 Production via AP-1. *The Journal of Immunology* **2011**, *187* (11), 6043–6051.
- 49. Li, R.; Fang, L.; Pu, Q.; Lin, P.; Hoggarth, A.; Huang, H.; Li, X.; Li, G.; Wu, M. Lyn Prevents Aberrant Inflammatory Responses to Pseudomonas Infection in Mammalian Systems by Repressing a SHIP-1-Associated Signaling Cluster. *Sig Transduct Target Ther* **2016**, *1* (1), 1–11.
- 50. Toubiana, J.; Rossi, A.-L.; Belaidouni, N.; Grimaldi, D.; Pene, F.; Chafey, P.; Comba, B.; Camoin, L.; Bismuth, G.; Claessens, Y.-E.; Mira, J.-P.; Chiche, J.-D. Src-Family-Tyrosine Kinase Lyn Is Critical for TLR2-Mediated NF-κB Activation through the PI 3-Kinase Signaling Pathway. *Innate Immun* **2015**, *21* (7), 685–697.
- 51. Avila, M.; Martinez-Juarez, A.; Ibarra-Sanchez, A.; Gonzalez-Espinosa, C. Lyn Kinase Controls TLR4-Dependent IKK and MAPK Activation Modulating the Activity of TRAF-6/TAK-1 Protein Complex in Mast Cells. *Innate Immun* **2012**, *18* (4), 648–660.
- 52. Yi, T.; Bolen, J. B.; Ihle, J. N. Hematopoietic Cells Express Two Forms of Lyn Kinase Differing by 21 Amino Acids in the Amino Terminus. *Molecular and Cellular Biology* **1991**, *11* (5), 2391–2398.
- 53. Freedman, T. S.; Tan, Y. X.; Skrzypczynska, K. M.; Manz, B. N.; Sjaastad, F. V.; Goodridge, H. S.; Lowell, C. A.; Weiss, A. LynA Regulates an Inflammation-Sensitive Signaling Checkpoint in Macrophages. *Elife* **2015**, *4*, e09183. DOI: 10.7554/eLife.09183
- 54. Brian, B. F., IV; Jolicoeur, A. S.; Guerrero, C. R.; Nunez, M. G.; Sychev, Z. E.; Hegre, S. A.; Sætrom, P.; Habib, N.; Drake, J. M.; Schwertfeger, K. L.; Freedman, T. S. Unique-Region Phosphorylation Targets LynA for Rapid Degradation, Tuning Its Expression and Signaling in Myeloid Cells. *eLife* **2019**, *8*, e46043. DOI: 10.7554/eLife.46043
- 55. Alvarez-Errico, D.; Yamashita, Y.; Suzuki, R.; Odom, S.; Furumoto, Y.; Yamashita, T.; Rivera, J. Functional Analysis of Lyn Kinase A and B Isoforms Reveals Redundant and Distinct Roles in Fc Epsilon RI-Dependent Mast Cell Activation. *J Immunol* **2010**, *184* (9), 5000–5008.
- 56. Brian, B. F., IV; Guerrero, C. R.; Freedman, T. S. Immunopharmacology and Quantitative Analysis of Tyrosine Kinase Signaling. *Current Protocols in Immunology* **2020**, *130* (1), e104. DOI: 10.1002/cpim.104
- 57. Livak, K. J.; Schmittgen, T. D. Analysis of Relative Gene Expression Data Using Real-Time Quantitative PCR and the 2(-Delta Delta C(T)) Method. *Methods* **2001**, 25 (4), 402–408.
- 58. Raza, S.; Barnett, M. W.; Barnett-Itzhaki, Z.; Amit, I.; Hume, D. A.; Freeman, T. C. Analysis of the Transcriptional Networks Underpinning the Activation of Murine Macrophages by Inflammatory Mediators. *J Leukoc Biol* **2014**, *96* (2), 167–183.
- 59. O'Connell, D. J.; Kolde, R.; Sooknah, M.; Graham, D. B.; Sundberg, T. B.; Latorre, I.; Mikkelsen, T. S.; Xavier, R. J. Simultaneous Pathway Activity Inference and Gene Expression Analysis Using RNA Sequencing. *Cell Syst* **2016**, *2* (5), 323–334.
- 60. Johannessen, L.; Sundberg, T. B.; O'Connell, D. J.; Kolde, R.; Berstler, J.; Billings, K. J.; Khor, B.; Seashore-Ludlow, B.; Fassl, A.; Russell, C. N.; Latorre, I. J.; Jiang, B.; Graham, D. B.; Perez, J. R.; Sicinski, P.; Phillips, A. J.; Schreiber, S. L.; Gray, N. S.; Shamji, A. F.; Xavier, R. J.

- Small-Molecule Studies Identify CDK8 as a Regulator of IL-10 in Myeloid Cells. *Nat Chem Biol* **2017**, *13* (10), 1102–1108.
- 61. Shi, H.; Sun, L.; Wang, Y.; Liu, A.; Zhan, X.; Li, X.; Tang, M.; Anderton, P.; Hildebrand, S.; Quan, J.; Ludwig, S.; Moresco, E. M. Y.; Beutler, B. N4BP1 Negatively Regulates NF-κB by Binding and Inhibiting NEMO Oligomerization. *Nat Commun* **2021**, *12*, 1379. DOI: 10.1038/s41467-021-21711-5
- 62. Kim, H. K.; De La Luz Sierra, M.; Williams, C. K.; Gulino, A. V.; Tosato, G. G-CSF down-Regulation of CXCR4 Expression Identified as a Mechanism for Mobilization of Myeloid Cells. *Blood* **2006**, 108 (3), 812–820.
- 63. House, I. G.; Savas, P.; Lai, J.; Chen, A. X. Y.; Oliver, A. J.; Teo, Z. L.; Todd, K. L.; Henderson, M. A.; Giuffrida, L.; Petley, E. V.; Sek, K.; Mardiana, S.; Gide, T. N.; Quek, C.; Scolyer, R. A.; Long, G. V.; Wilmott, J. S.; Loi, S.; Darcy, P. K.; Beavis, P. A. Macrophage-Derived CXCL9 and CXCL10 Are Required for Antitumor Immune Responses Following Immune Checkpoint Blockade. *Clinical Cancer Research* **2020**, 26 (2), 487–504.
- 64. Liu, H.; Zhu, T.; Li, Q.; Xiong, X.; Wang, J.; Zhu, X.; Zhou, X.; Zhang, L.; Zhu, Y.; Peng, Y.; Chen, Y.; Hu, C.; Chen, H.; Guo, A. TRIM25 Upregulation by Mycobacterium Tuberculosis Infection Promotes Intracellular Survival of M.Tb in RAW264.7 Cells. *Microbial Pathogenesis* **2020**, 148, 104456. DOI: 10.1016/j.micpath.2020.104456
- 65. Bian, Z.; Shi, L.; Guo, Y.-L.; Lv, Z.; Tang, C.; Niu, S.; Tremblay, A.; Venkataramani, M.; Culpepper, C.; Li, L.; Zhou, Z.; Mansour, A.; Zhang, Y.; Gewirtz, A.; Kidder, K.; Zen, K.; Liu, Y. Cd47-Sirpα Interaction and IL-10 Constrain Inflammation-Induced Macrophage Phagocytosis of Healthy Self-Cells. *Proceedings of the National Academy of Sciences* **2016**, 113 (37), E5434–E5443. DOI: 10.1073/pnas.1521069113
- 66. Liberzon, A.; Birger, C.; Thorvaldsdóttir, H.; Ghandi, M.; Mesirov, J. P.; Tamayo, P. The Molecular Signatures Database Hallmark Gene Set Collection. *Cell Systems* **2015**, *1* (6), 417–425.
- 67. Scapini, P.; Pereira, S.; Zhang, H.; Lowell, C. A. Multiple Roles of Lyn Kinase in Myeloid Cell Signaling and Function. *Immunological Reviews* **2009**, *228* (1), 23–40.
- 68. Harder, K. W.; Parsons, L. M.; Armes, J.; Evans, N.; Kountouri, N.; Clark, R.; Quilici, C.; Grail, D.; Hodgson, G. S.; Dunn, A. R.; Hibbs, M. L. Gain- and Loss-of-Function Lyn Mutant Mice Define a Critical Inhibitory Role for Lyn in the Myeloid Lineage. *Immunity* **2001**, *15* (4), 603–615.
- 69. Roberts, M. E.; Barvalia, M.; Silva, J. A. F. D.; Cederberg, R. A.; Chu, W.; Wong, A.; Tai, D. C.; Chen, S.; Matos, I.; Priatel, J. J.; Cullis, P. R.; Harder, K. W. Deep Phenotyping by Mass Cytometry and Single-Cell RNA-Sequencing Reveals LYN-Regulated Signaling Profiles Underlying Monocyte Subset Heterogeneity and Lifespan. *Circulation Research* **2020**, *126* (10), e61–e79. DOI: 10.1161/CIRCRESAHA.119.315708
- 70. Gautier, E. L.; Ivanov, S.; Lesnik, P.; Randolph, G. J. Local Apoptosis Mediates Clearance of Macrophages from Resolving Inflammation in Mice. *Blood* **2013**, 122 (15), 2714–2722.
- 71. Henke, E.; Nandigama, R.; Ergün, S. Extracellular Matrix in the Tumor Microenvironment and Its Impact on Cancer Therapy. *Frontiers in Molecular Biosciences* **2020**, *6*, 160. DOI: 10.3389/fmolb.2019.00160
- 72. Di Martino, J. S.; Nobre, A. R.; Mondal, C.; Taha, I.; Farias, E. F.; Fertig, E. J.; Naba, A.; Aguirre-Ghiso, J. A.; Bravo-Cordero, J. J. A Tumor-Derived Type III Collagen-Rich ECM Niche Regulates Tumor Cell Dormancy. *Nat Cancer* **2022**, *3* (1), 90–107.
- 73. Nguyen, P.-H.; Fedorchenko, O.; Rosen, N.; Koch, M.; Barthel, R.; Winarski, T.; Florin, A.; Wunderlich, F. T.; Reinart, N.; Hallek, M. LYN Kinase in the Tumor Microenvironment Is Essential for the Progression of Chronic Lymphocytic Leukemia. *Cancer Cell* **2016**, *30* (4), 610–622.
- 74. vom Stein, A. F.; Rebollido-Rios, R.; Lukas, A.; Koch, M.; von Lom, A.; Reinartz, S.; Bachurski, D.; Rose, F.; Bozek, K.; Abdallah, A. T.; Kohlhas, V.; Saggau, J.; Zölzer, R.; Zhao, Y.; Bruns, C.; Bröckelmann, P. J.; Lohneis, P.; Büttner, R.; Häupl, B.; Oellerich, T.; Nguyen, P.-H.; Hallek, M. LYN Kinase Programs Stromal Fibroblasts to Facilitate Leukemic Survival via Regulation of C-JUN and THBS1. *Nat Commun* **2023**, *14* (1), 1330. DOI: 10.1038/s41467-023-36824-2

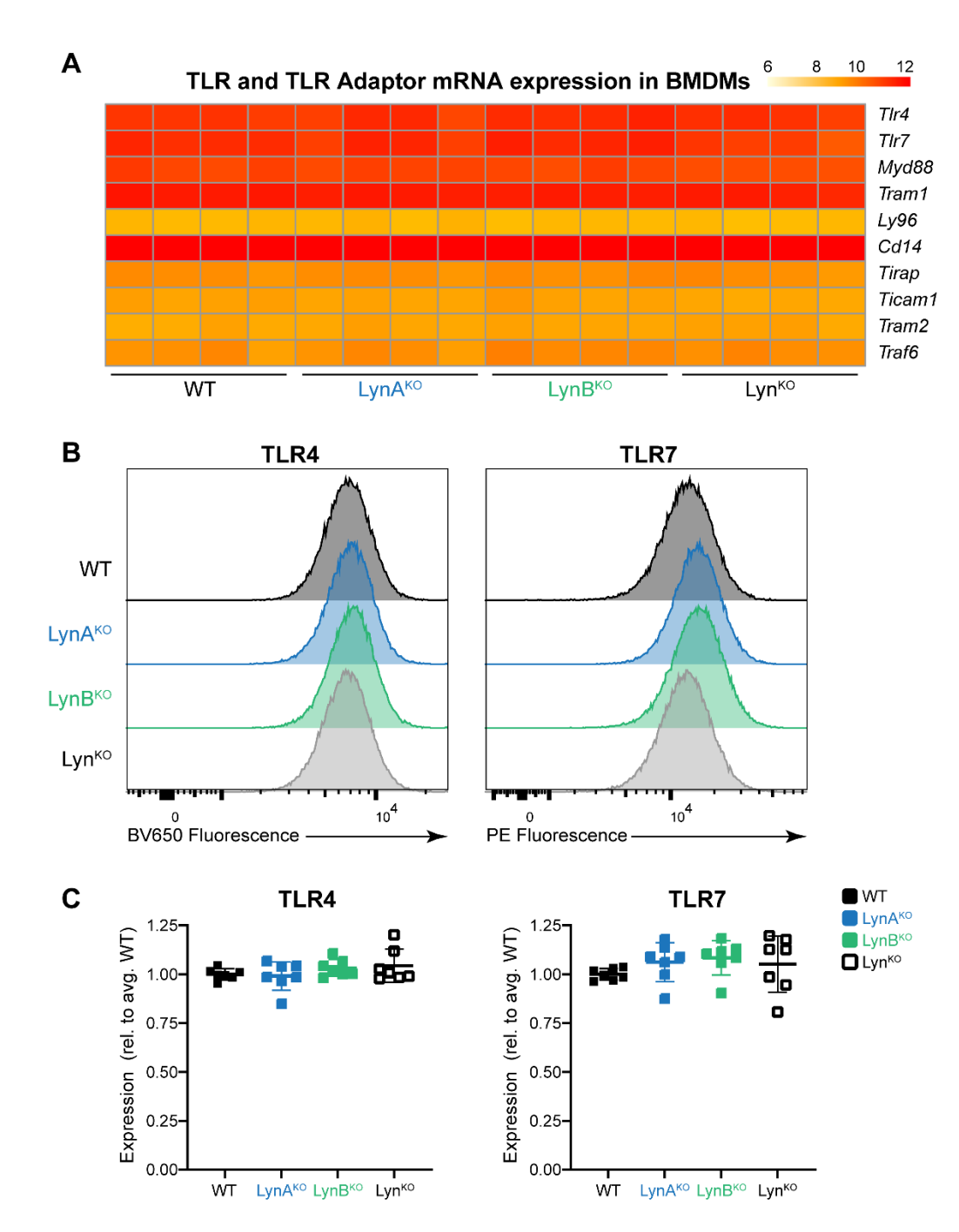
- 75. Iqbal, M. S.; Tsuyama, N.; Obata, M.; Ishikawa, H. A novel signaling pathway associated with Lyn, PI 3-kinase and Akt supports the proliferation of myeloma cells. *Biochem Biophys Res Commun* **2010**, 392 (3): 415–20.
- 76. Tsantikos, E.; Maxwell, M. J.; Kountouri, N.; Harder, K. W.; Tarlinton, D. M.; Hibbs, M. L. Genetic Interdependence of Lyn and Negative Regulators of B Cell Receptor Signaling in Autoimmune Disease Development. *J Immunol* **2012**, *189* (4), 1726–1736.



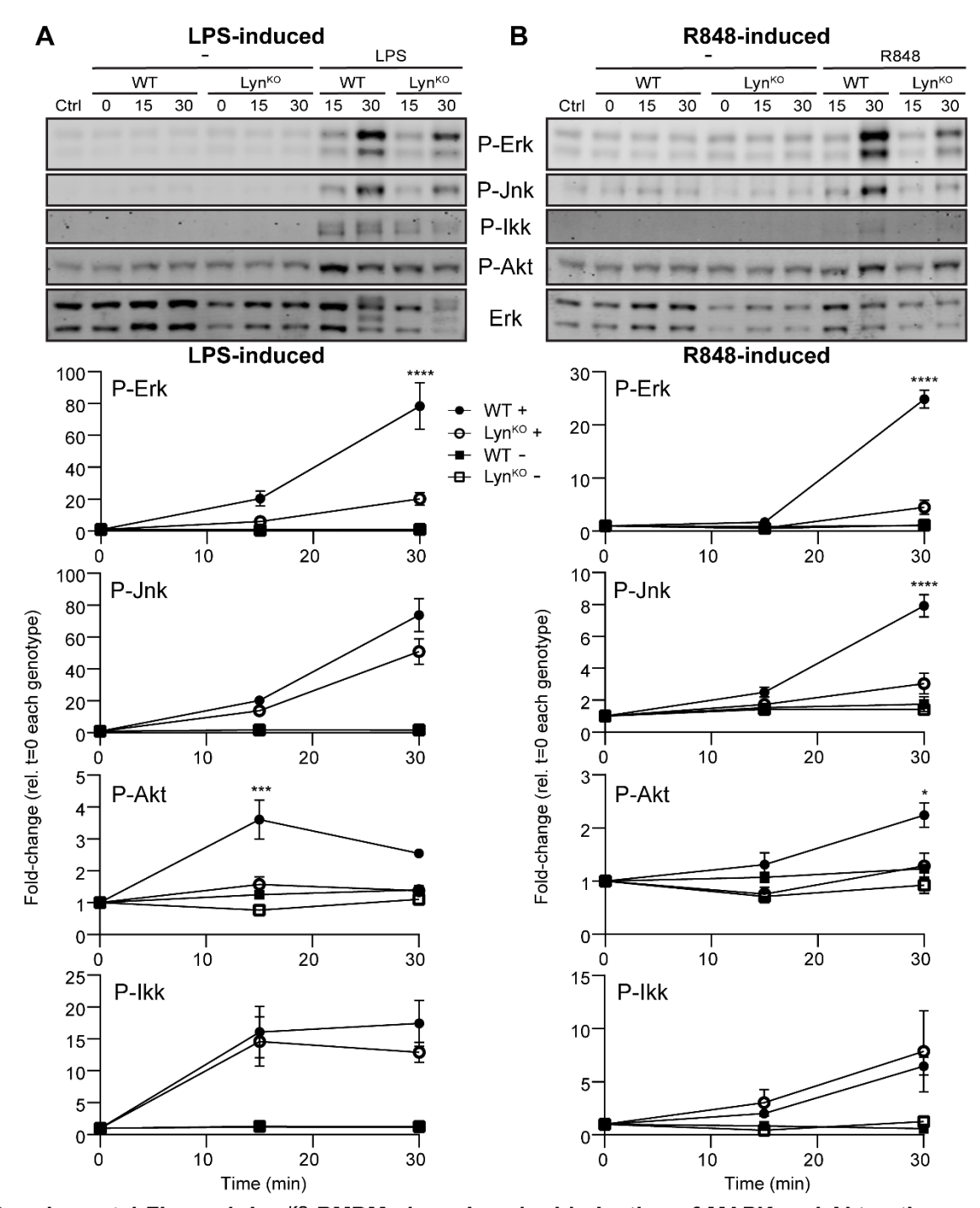
Supplemental Figure 1. WT, LynA^{KO}, and LynB^{KO} BMDMs have few transcriptomic differences. Heat maps with all significant DEGs between WT and either LynA^{KO} or LynB^{KO} BMDMs (A) at steady state or (B-C) after 2 h LPS or R848 treatment. (B) DEGs similarly upregulated or downregulated by after treatment with TLR agonist. (C) DEGs specific to LPS or R848 treatment. Heat maps and DEGs were compiled as described in Fig. 2.



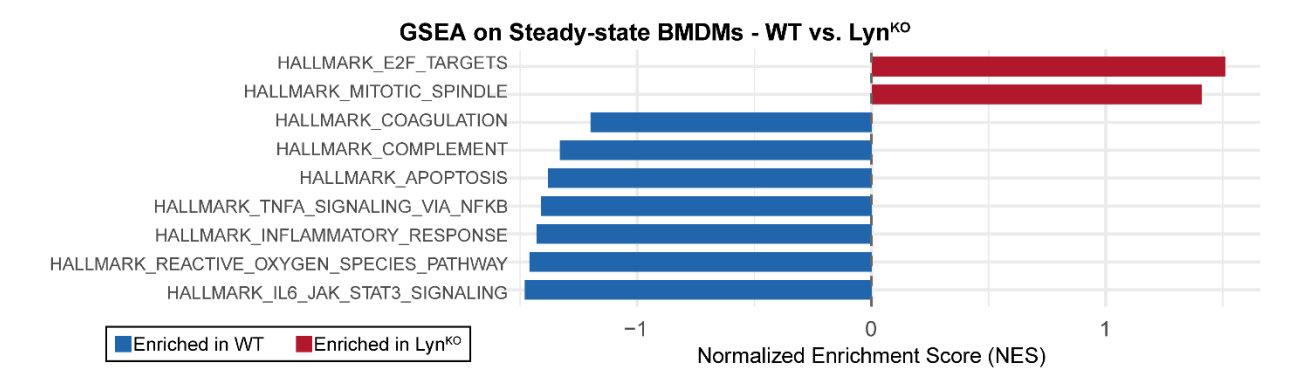
Supplemental Figure 2. LPS and R848 have differential impacts on gene transcription in WT BMDMs. (A inset) qRT-PCR analysis of Tnf expression in response to 2 h treatment with 2 ng/ml LPS or 20 ng/ml R848. Significance was assessed via one-way ANOVA with Tukey's multiple comparisons test: ***P = 0.0002-0.0003. There was no significant difference (ns) between LPS and R848 conditions (P=0.9669). (A-C) Volcano plots highlighting DEGs in (A) LPS- or R848-treated WT BMDMs relative to each other, (B) LPS-treated relative to steady-state, or (C) R848-treated relative to steady-state. DEGs were calculated as described in Fig. 2.

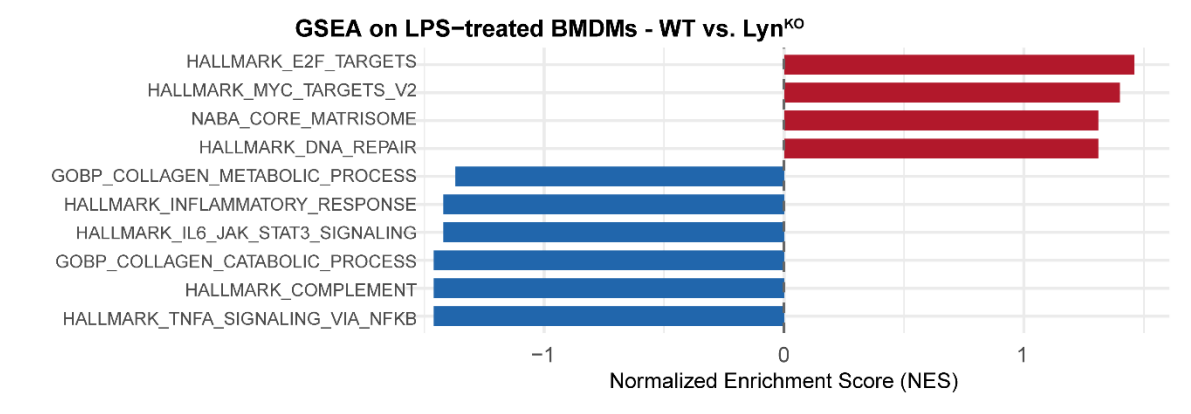


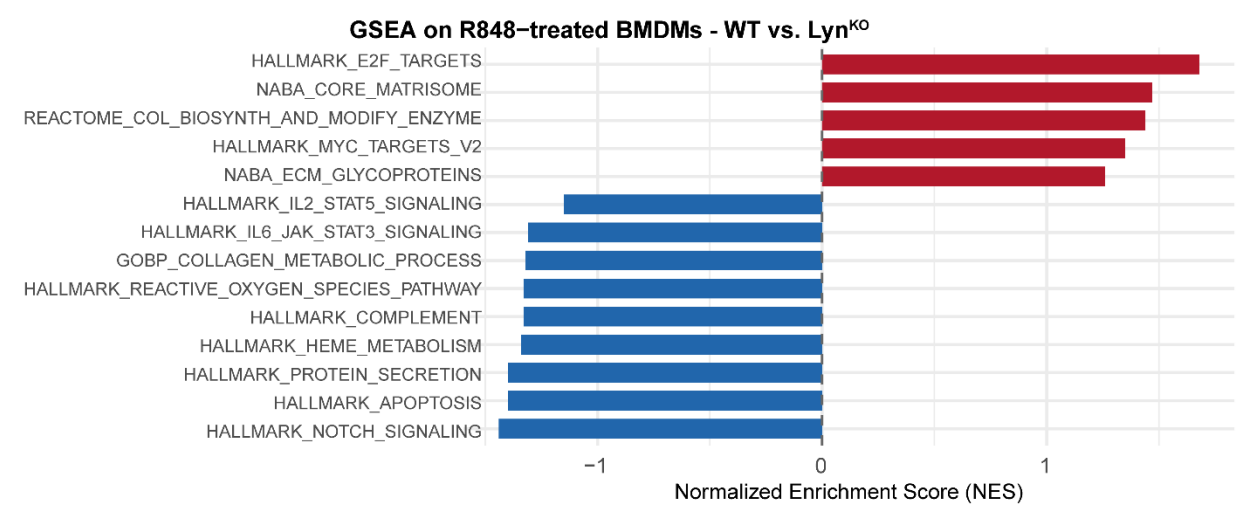
Supplemental Figure 3. Lyn knockout does not affect TLR4 or TLR7 expression by BMDMs. (A) RNA-sequencing data showing VST-normalized hit-counts of Tlr4, Tlr7, and TLR adaptors in BMDMs at steady state (red: higher expression). (B) Representative flow-cytometry histograms showing protein expression of surface TLR4 and intracellular TLR7 in BMDMs. (C) Quantified flow-cytometry data showing relative TLR expression in WT and Lyn-deficient BMDMs, comparing the geometric mean fluorescent intensity for each sample to that of WT within each experiment (n=7 biological replicates over 3 experimental days). No significant differences were observed.



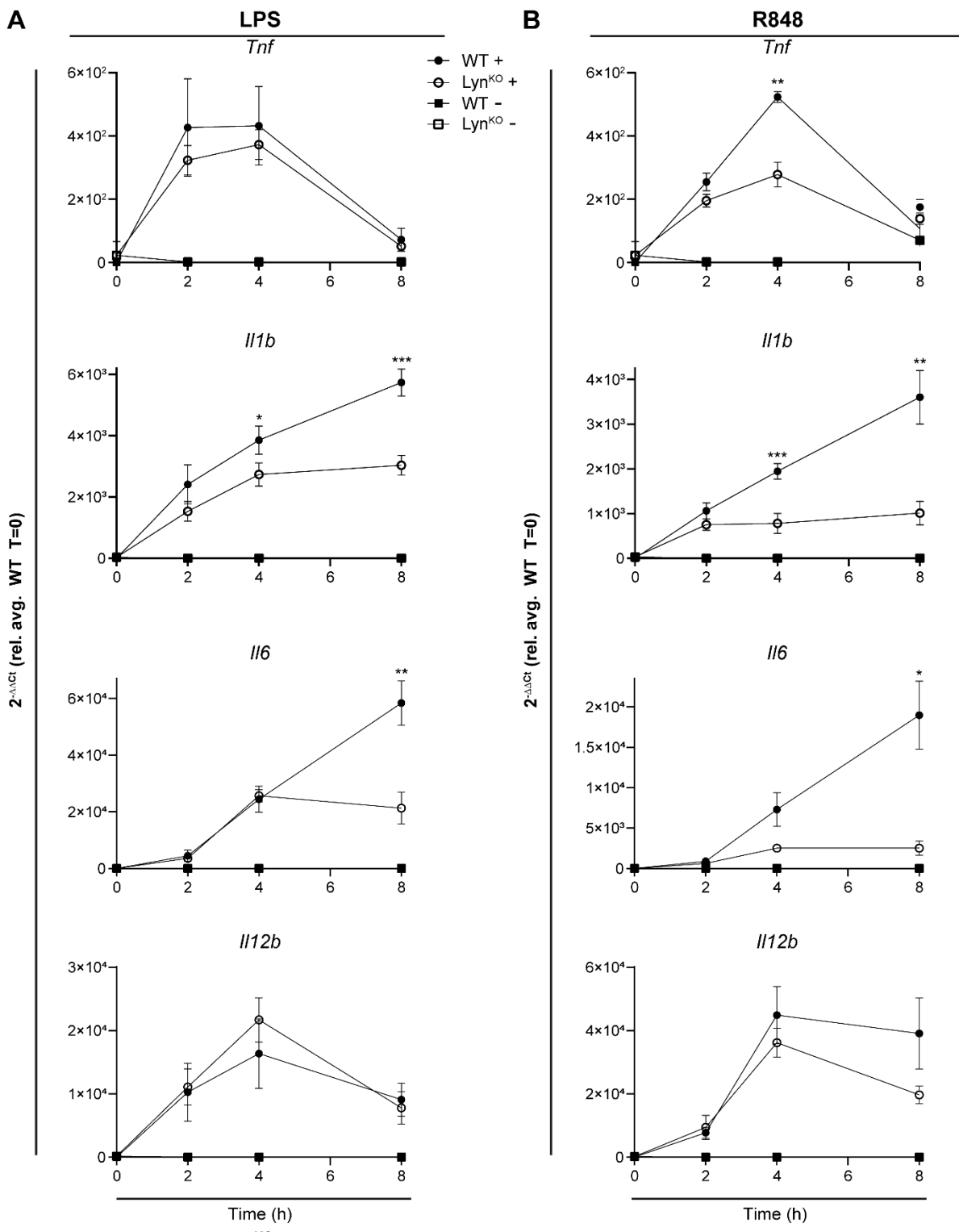
Supplemental Figure 4. Lyn^{KO} **BMDMs have impaired induction of MAPK and Akt pathways after TLR4 and TLR7 stimulation.** Representative immunoblots showing phosphorylation of downstream signaling proteins in WT and Lyn^{KO} BMDMs at steady state and after 15 and 30 min treatment with **(A)** 2 ng/ml LPS or **(B)** 20 ng/ml R848. Lysates from BMDMs treated with agonist (+) or medium alone (-) are shown. Quantifications of P-Erk, P-Jnk, P-lkk, and P-Akt are corrected for total protein staining in each gel lane and shown relative to the untreated t=0 sample within each genotype (n=4). Total Erk reflects protein loading. Data are presented as mean ± SEM. Significance was assessed via two-way ANOVA comparing WT and Lyn^{KO} agonist-treated cells with Tukey's multiple comparisons test. p <0.05 *, <0.01 **, <0.001 ****, <0.0001 *****, with no significant differences other than those indicated. n indicates the number of biological replicates, with cells from different individual mice.







Supplemental Figure 5. Enrichment of cell-cycle and matrix-assembly pathways in Lyn^{KO} BMDMs and enrichment of inflammatory and catabolic pathways in WT. Graphical summary of GSEA performed on RNA-sequencing data from WT and Lyn^{KO} BMDMs at steady state and after LPS or R848 treatment (n=4). Bar plots show normalized enrichment scores (NES) for significantly enriched pathways identified using GSEA, with hallmark and curated gene sets from the MSigDB. Positive NES values (red) indicate enrichment in Lyn^{KO}; negative NES values (blue) indicate enrichment in WT. Significance was defined by a nominal p-value <0.1. n indicates the number of biological replicates per genotype (each from a different mouse) and treatment.



Supplemental Figure 6. Lyn^{KO} BMDMs have a defect in maximum cytokine induction rather than a kinetic defect. (A-B) qRT-PCR showing Tnf, II1b, II6, and II12b expression by WT and total Lyn^{KO} BMDMs at steady state (-) and after 2, 4, and 8 h treatment (+) with (A) 2 ng/ml LPS or (B) 20 ng/ml R848 (n=4). Data are presented as mean \pm SEM. Significance was assessed via two-way ANOVA with Tukey's multiple comparisons test. p-value <0.05 *, <0.01 ***, <0.001 ****, <0.0001 *****, with all other pairwise comparisons lacking significant differences. n is the number of biological replicates, with cells from different mice.